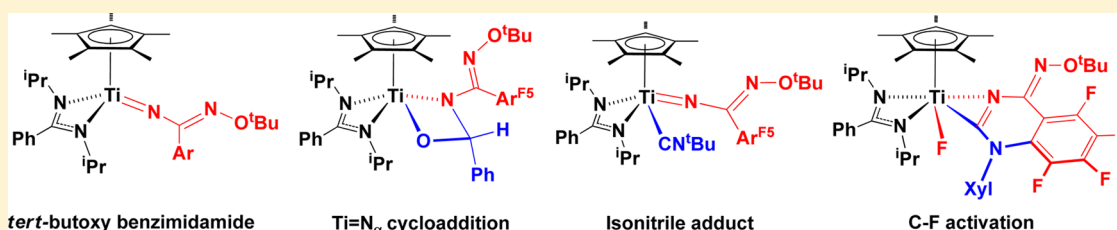


Reactions of a Cyclopentadienyl–Amidinate Titanium Benzimidamido Complex

Laura R. Groom, Adam F. Russell, Andrew D. Schwarz, and Philip Mountford*

Chemistry Research Laboratory, Department of Chemistry, University of Oxford, Mansfield Road, Oxford OX1 3TA, U.K.

S Supporting Information



ABSTRACT: We report the first reactivity study of a transition-metal benzimidamido complex, namely Cp*Ti{PhC(NⁱPr)₂}{NC(Ar^{F5})NO^tBu} (**5**, Ar^{F5} = C₆F₅). Reaction with CO₂ and ^tBuNCO gave the cycloaddition products Cp*Ti{PhC(NⁱPr)₂}{OC(O)N(C{Ar^{F5}}NO^tBu)} and Cp*Ti{PhC(NⁱPr)₂}{OC(N^tBu)N(C{Ar^{F5}}NO^tBu)} (**10**), respectively, whereas with CS₂ slow extrusion of Ar^{F5}CN from **5** occurred to ultimately form Cp*Ti{PhC(NⁱPr)₂}{SC(S)N(O^tBu)}. Reaction of **5** with ArC(O)H (Ar = Ph, 4-C₆H₄Me, 4-C₆H₄^tBu, 4-C₆H₄OMe, 4-C₆H₄NMe₂, 4-C₆H₄CF₃) also gave the isolable metallacyclic complexes Cp*Ti{PhC(NⁱPr)₂}{N(C{Ar^{F5}}NO^tBu)C(Ar)(H)O} (**13**) via reversible [2 + 2] cycloaddition reactions. In contrast, reaction with HC(O)NMe₂ formed Me₂N{NC(Ar^{F5})NO^tBu}H (**16**) within 1 h at room temperature. Upon heating, **10** and **13** also underwent retrocyclization, forming the organic products ^tBuNCNC(Ar^{F5})NO^tBu and ArC{NC(Ar^{F5})NO^tBu}H (**14**), respectively. Selected examples of **14** and **16** were studied by DFT and UV–visible spectroscopy. Addition of isonitriles ^tBuNC and XylNC (Xyl = 2,6-C₆H₃Me₂) to Cp*Ti{PhC(NⁱPr)₂}{NC(Ar)NO^tBu} (Ar = Ar^{F5} (**5**), 2,6-C₆H₃F₂ (Ar^{F2})) afforded the σ-adducts Cp*Ti{PhC(NⁱPr)₂}{NC(Ar)NO^tBu}{CNR} (Ar = Ar^{F5}, R = ^tBu, Xyl (**19**); Ar = Ar^{F2}, R = Xyl). Subsequently, **19** formed Cp*Ti{PhC(NⁱPr)₂}{NC(NO^tBu)C₆F₄N(Xyl)C}(F) (**20**) via C–F bond activation. Reaction of **5** with 2 equiv of B(Ar^{F5})₃ gave Cp*Ti{PhC(NⁱPr)₂}{ON(B{Ar^{F5}}₃)C(Ar^{F5})N(H)(B{Ar^{F5}}₃)} with elimination of 2-methylpropene.

INTRODUCTION

During the past 20 years, the chemistry of group 4 imido complexes¹ (L)M=NR (R = alkyl, aryl) and, more recently, hydrazido complexes (L)M=NNR₂ (M = Ti,² Zr³ in particular) has been extensively developed. The structure and bonding of these complexes is well-established. The unsaturated M=N multiple bonds (formally σ²π⁴ triple bonds in most instances^{21,t,4}) normally act as the reactive site in imido and hydrazido complexes and undergo a wide range of addition reactions with saturated and, especially, unsaturated substrates. In some instances, imides act only as supporting or spectator ligands: for example, in the context of olefin polymerization.⁵ In addition to M=N_α bond reactivity, it has been shown that group 4 hydrazido complexes can also undergo reductive cleavage (e.g., with CO^{3a} and isonitriles^{2s,z,3b}) or reductive insertion reactions of the N_α–N_β bonds (with alkynes^{21,q,z,3n}). The mechanism^{2q,3j,n} of alkyne insertion into the N_α–N_β bond of certain titanium and zirconium hydrazides is related to that for reductive cleavage of the peroxide ligand O_α–O_β bond in Cp*₂Hf(R)(OO^tBu) to form Cp*₂Hf(OR)(O^tBu) (R = H, alkyl).⁶ Following on from these studies, we have therefore started to explore the chemistry of titanium alkoxyimido complexes, (L)Ti=NO^tR,⁷ with the aim of developing both new Ti=N_α multiple-bond chemistry as well as N_α–O_β bond

reactivity. Indeed, the reaction chemistry of alkoxyimides in general is still virtually unexplored.⁸ As part of this research program,^{7c} we recently synthesized the *tert*-butoxyimido complexes Cp*Ti{RC(NⁱPr)₂}{NO^tBu} (**1**; R = Me, Ph) (Figure 1), supported by the cyclopentadienyl–amidinate ligand set. This robust ligand platform was chosen as it was used very successfully in the past to study the reactivity of a range of imido,⁹ hydrazido,^{21,r,u,v,x} and alkyldiene hydrazido (i.e., (L)Ti=NNCRR')^{4g} complexes, therefore allowing meaningful comparisons with these related functional groups.

The Ti=NO^tBu moiety of **1** undergoes a number of new transformations for this type of functional group, including [2 + 2] cycloaddition reactions with CS₂ and Ar'NCO (forming **2**, Figure 1; Ar' = 2,6-C₆H₃Pr₂), a double-addition reaction with TolNCO, coupling of substrate, net NO^tBu group transfer with ^tBuNCO and PhC(O)R (R = H, Me, Ph) via C=O/Ti=N_α metathesis, reductive N_α–O_β bond cleavage with Ar^{F5}CCH (Ar^{F5} = C₆F₅), and formation of an unusual nitroxyl (HNO) complex upon reaction with B(Ar^{F5})₃ with concomitant 2-methylpropene elimination.^{7c} Of particular relevance to our current contribution are the reactions of **1**

Received: December 5, 2013

Published: February 3, 2014

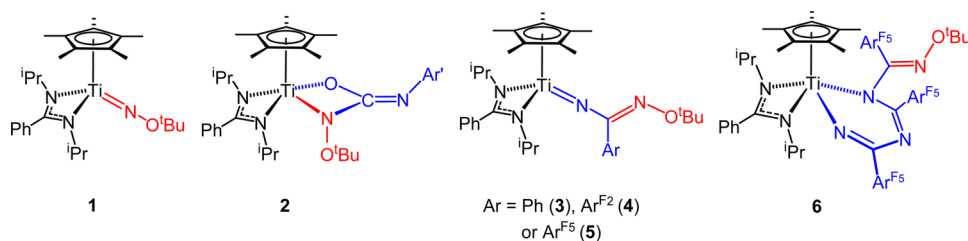


Figure 1. $\text{Cp}^*\text{Ti}\{\text{PhC}(\text{N}^i\text{Pr})_2\}(\text{NO}^t\text{Bu})$ (**1**) and its reaction products with $\text{Ar}'\text{NCO}$ and benzonitriles. Atoms from the NO^tBu ligand are shown in red, and those from the organic substrates are shown in blue. $\text{Ar}' = 2,6\text{-C}_6\text{H}_3\text{Pr}_2$.

with benzonitriles to form the net $\text{Ti}=\text{N}_\alpha$ bond insertion products $\text{Cp}^*\text{Ti}\{\text{PhC}(\text{N}^i\text{Pr})_2\}\{\text{NC}(\text{Ar})\text{NO}^t\text{Bu}\}$ ($\text{Ar} = \text{Ph}$ (**3**), $\text{C}_6\text{H}_3\text{F}_2$ (Ar^{F_2} , **4**), Ar^{F_5} (**5**)) containing new benzimidamido functional groups, i.e. $\text{Ti}=\text{NC}(\text{Ar})\text{NO}^t\text{Bu}$ (Figure 1), also possessing a formal $\text{Ti}\equiv\text{N}$ $\sigma^2\pi^4$ triple bond. The stability of these complexes increases in the order $\text{Ar} = \text{Ph}$ (**3**) < Ar^{F_2} (**4**) < Ar^{F_5} (**5**) as the aryl groups become better able to stabilize the electron-rich multiple bond. Although the reactions of nitriles with transition-metal nitrides,¹⁰ alkylidenes,¹¹ and alkylidynes¹² are very well established, their reactions with transition-metal imides and hydrazides are still relatively uncommon,^{2q,s,z,4g,13} and the reaction chemistry of the benzimidamido ligand has therefore remained unexplored. Encouragingly in this regard, compound **5** reacted with an excess of $\text{Ar}^{\text{F}_5}\text{CN}$ to form **6** (Figure 1), containing two additional benzonitrile units. This was the first example of any reaction of an isolated benzimidamido complex and only the second example of the double addition of nitriles across a $\text{M}=\text{NR}$ bond. The first example was the very recently reported head-to-tail coupling of 2 equiv of ArCN across the $\text{Ti}=\text{N}(\text{N}(\text{CPh}_2))_2$ bond of the alkylidene hydrazide $\text{Cp}^*\text{Ti}\{\text{MeC}(\text{N}^i\text{Pr})_2\}(\text{N}(\text{N}(\text{CPh}_2))_2)$, forming $\text{Cp}^*\text{Ti}\{\text{MeC}(\text{N}^i\text{Pr})_2\}(\text{N}(\text{N}(\text{CPh}_2))_2)\text{C}(\text{Ar})\text{NC}(\text{Ar})\text{N}$ ($\text{Ar} = \text{Ph}$, Ar^{F_5}).^{4g} The only related example of a similar double addition of nitriles was reported for the transient oxo and sulfido complexes $\text{Cp}^*_2\text{Zr}(\text{E})$ ($\text{E} = \text{O}, \text{S}$).¹⁴

The reaction of **5** with further equivalents of $\text{Ar}^{\text{F}_5}\text{CN}$ prompted us to develop this compound's reaction chemistry with other substrates. This would also, in effect, result in multiple substrate/cross-coupling reactions of the $\text{Ti}=\text{NO}^t\text{Bu}$ functional group of **1**. Interestingly, while multiple couplings of CO_2 ,^{2e,v,9a,d} isocyanates,^{2v,4g,9d} and alkynes,¹⁵ and of an alkyne and a nitrile^{2s} or isonitrile^{2e} across a number of $\text{Ti}=\text{N}_\alpha\text{R}$ ($\text{R} = \text{hydrocarbyl}, \text{NR}_2, \text{N}(\text{CPh}_2), \text{NO}^t\text{Bu}$) bonds are known, these predominantly involve insertion of the second substrate into the single $\text{Ti}-\text{X}$ bond ($\text{X} = \text{N}, \text{C}$) of an initial $[2 + 2]$ cycloaddition intermediate (for example of the type **2** in Figure 1). Multiple substrate coupling starting from **1** and nitriles would follow a different mechanistic paradigm, with each stage involving substrate addition to a metal–nitrogen multiple bond (i.e., $\text{Ti}=\text{NO}^t\text{Bu}$ followed by $\text{Ti}=\text{NC}(\text{Ar})\text{NO}^t\text{Bu}$). In this contribution we report our studies of the reactions of $\text{Cp}^*\text{Ti}\{\text{PhC}(\text{N}^i\text{Pr})_2\}\{\text{NC}(\text{Ar}^{\text{F}_5})\text{NO}^t\text{Bu}\}$ (**5**) with heterocumulenes, aldehydes, dimethyl formamide, isonitriles, and $\text{B}(\text{Ar}^{\text{F}_5})_3$.

RESULTS AND DISCUSSION

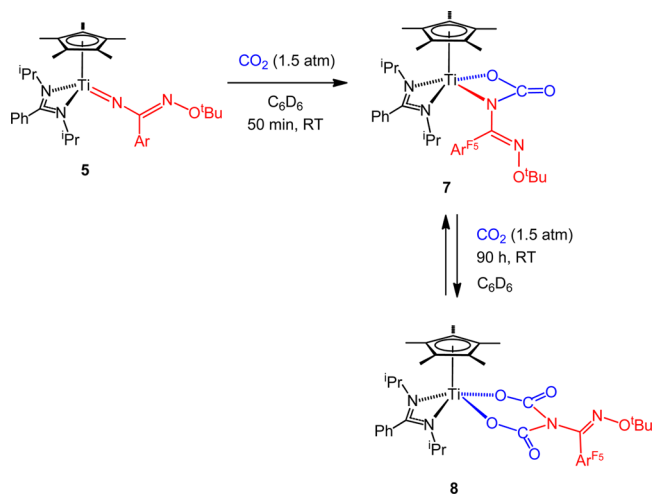
The benzimidamido compounds $\text{Cp}^*\text{Ti}\{\text{PhC}(\text{N}^i\text{Pr})_2\}\{\text{NC}(\text{Ar})\text{NO}^t\text{Bu}\}$ ($\text{Ar} = \text{Ar}^{\text{F}_2}$ (**4**), Ar^{F_5} (**5**)) are readily formed from $\text{Cp}^*\text{Ti}\{\text{PhC}(\text{N}^i\text{Pr})_2\}(\text{NO}^t\text{Bu})$ (**1**) and the corresponding nitrile, and when they are followed on the NMR tube scale the conversions are quantitative and effectively immediate in the case of **5**.^{7c} However, owing to its high solubility in aliphatic

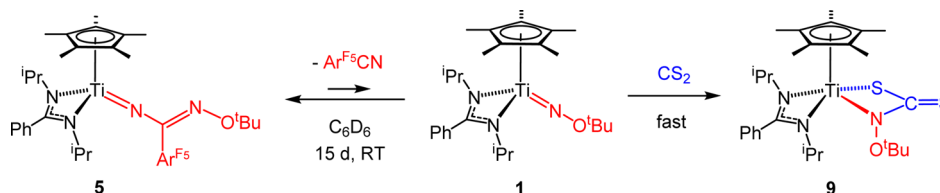
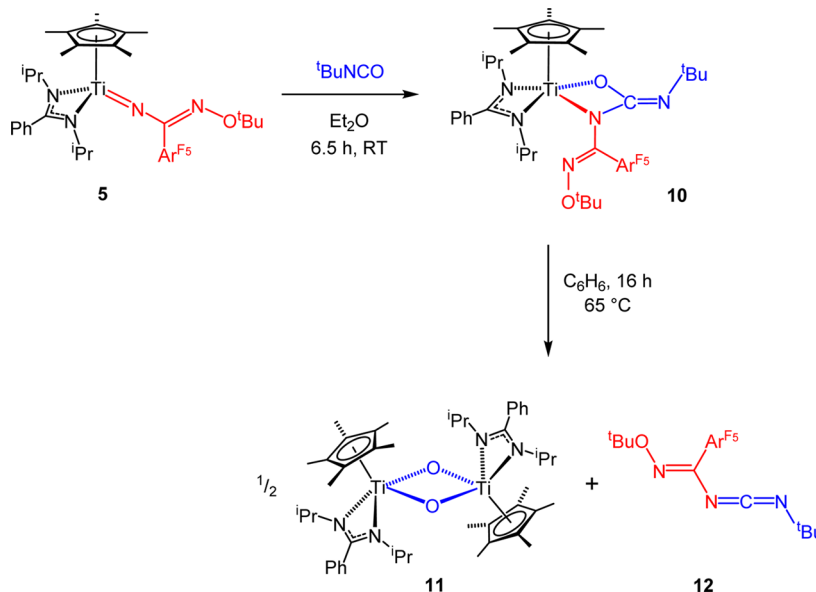
solvents, **5** could only be isolated in less than 35% yield on a preparative scale. Therefore, in the following chemistry **5** was generally generated in situ for reasons of efficiency. When reactions of formally isolated **5** were compared with those of the in situ generated system, no differences were observed.

Reactions with Heterocumulenes. The influence of N_α substituents, $(\text{L})\text{Ti}=\text{N}_\alpha-\text{X}$, on the reactivity of titanium imido and hydrazido complexes with CO_2 , CS_2 , and isocyanates is well established,^{1c-e,2b,k,n,v,z,4g,9c-e} and initial studies of alkoxyimido complexes have shown behavior similar to that of their hydrazido and imido counterparts.^{4g,7c} A $[2 + 2]$ cycloaddition product is the key intermediate in all reactions with these substrates. However, there are relatively few examples where these intermediates are observed or (especially) isolated. Their unstable nature often leads to extrusion (via retrocyclization) of an organic fragment, leaving behind a titanium oxo species which, unless trapped, rapidly dimerizes via μ -oxo bridge formation. We were therefore interested to explore the reactions of $\text{Cp}^*\text{Ti}\{\text{PhC}(\text{N}^i\text{Pr})_2\}\{\text{NC}(\text{Ar}^{\text{F}_5})\text{NO}^t\text{Bu}\}$ (**5**) with heterocumulenes, in particular since the electron-withdrawing nature of the C_6F_5 substituent should help to stabilize these intermediates.

When the reaction of **5** with an excess of CO_2 (ca. 1.5 atm) was followed by NMR spectroscopy, quantitative conversion to compound **7** was observed within 50 min at room temperature (Scheme 1). Compound **7** was isolated on the preparative scale in 66% yield and characterized by NMR and IR spectroscopy and elemental analysis. The NMR and other data are characteristic of the C_1 -symmetric $[2 + 2]$ cycloaddition product $\text{Cp}^*\text{Ti}\{\text{PhC}(\text{N}^i\text{Pr})_2\}\{\text{OC}(\text{O})\text{N}(\text{C}\{\text{Ar}^{\text{F}_5}\}\text{NO}^t\text{Bu})\}$

Scheme 1. Reaction of $\text{Cp}^*\text{Ti}\{\text{PhC}(\text{N}^i\text{Pr})_2\}\{\text{NC}(\text{Ar}^{\text{F}_5})\text{NO}^t\text{Bu}\}$ (**5**) with CO_2



Scheme 2. Reaction of $\text{Cp}^*\text{Ti}\{\text{PhC}(\text{N}^i\text{Pr})_2\}\{\text{NC}(\text{Ar}^{\text{F}_5})\text{NO}^t\text{Bu}\}$ (**5**) with CS_2 Scheme 3. Reaction of $\text{Cp}^*\text{Ti}\{\text{PhC}(\text{N}^i\text{Pr})_2\}\{\text{NC}(\text{Ar}^{\text{F}_5})\text{NO}^t\text{Bu}\}$ (**5**) with $^t\text{BuNCO}$ 

(7), containing a N,O-bound carbamate-type ligand. For example, two apparent septets are observed in the ^1H NMR spectrum for the inequivalent isopropyl groups, along with four doublets for the two pairs of diastereotopic methyl groups. The ^{19}F NMR spectrum shows five new resonances (range $\delta -137.7$ to -164.9 ppm), which indicates restricted rotation about the C– C_{ipso} bond to the C_6F_5 ring. The ^{13}C NMR C=O resonance at $\delta 155.8$ ppm is similar to the corresponding values for $\text{Cp}^*\text{Ti}\{\text{MeC}(\text{N}^i\text{Pr})_2\}\{\text{OC}(\text{O})\text{N}(\text{NR}_2)\}$ (R = Ph, $\delta 160.6$ ppm; R = Me, $\delta 158.1$ ppm).^{2v} The IR spectra of **7** and these compounds all show strong $\nu(\text{C}=\text{O})$ bands at 1690, 1684, and 1667 cm^{-1} , respectively, for the carbamate ligands.

Like its arylimido-^{9d} and hydrazido-^{2v} derived counterparts, compound **7** does not undergo retro-cyclization to eliminate $^t\text{BuONC}(\text{Ar}^{\text{F}_5})\text{NCO}$, and is stable for many days in solution at room temperature. However, in the presence of an excess of CO_2 , **7** eventually forms the C_s -symmetric “double-insertion” product $\text{Cp}^*\text{Ti}\{\text{PhC}(\text{N}^i\text{Pr})_2\}\{\text{OC}(\text{O})\text{N}(\text{C}\{\text{Ar}^{\text{F}_5}\}\text{NO}^t\text{Bu})\text{C}(\text{O})\text{O}\}$ (**8**, Scheme 1). The reaction is slow, and when followed in C_6D_6 reaches only 70% conversion after ca. 90 h, at which stage no further reaction is observed. Upon heating the reaction mixture or attempted isolation, compound **8** eliminates CO_2 reforming **7**. The reversible insertion of a heterocumulene into the Ti–N bond of a metallacyclic species such as **7** has been observed previously.^{2b} Compound **8** was characterized *in situ* by ^1H , ^{13}C and ^{19}F NMR spectroscopy. The ^1H NMR spectrum shows one septet corresponding to the equivalent isopropyl methine hydrogens, and two doublets for the methyl groups of these substituents. The ^{13}C NMR spectrum shows a shift in the C=O and $\text{NC}(\text{Ar}^{\text{F}_5})\text{N}$ resonances from $\delta 155.8$ to 152.8 ppm and from $\delta 146.2$ to 137.3 ppm, respectively. The

related compounds $\text{Cp}^*\text{Ti}\{\text{MeC}(\text{N}^i\text{Pr})_2\}\{\text{OC}(\text{O})\text{N}(\text{NR}_2)\text{C}(\text{O})\text{O}\}$ (R = Me, Ph) show corresponding C=O resonances at $\delta 152.8$ and 152.7 ppm, respectively, which are also shifted to higher field in comparison to their respective cycloaddition precursors.^{2v}

Reaction of **5** with a small excess of CS_2 in C_6D_6 resulted in the very slow formation of the known^{7c} compound $\text{Cp}^*\text{Ti}\{\text{PhC}(\text{N}^i\text{Pr})_2\}\{\text{SC}(\text{S})\text{N}(\text{O}^t\text{Bu})\}$ (**9**; Scheme 2) and $\text{Ar}^{\text{F}_5}\text{CN}$, and after 15 days at room temperature the reaction had still only reached ca. 65% conversion. At this stage significant amounts of unknown side products were present in the ^1H NMR spectrum. The amount of these increased upon heating at 70 °C. The reaction probably proceeds via slow extrusion of $\text{Ar}^{\text{F}_5}\text{CN}$ from **5**, yielding the alkoxyimido compound **1** (not observed) which, as previously reported, reacts relatively quickly with CS_2 to form the apparently more stable cycloaddition product **9**.^{7c} The extrusion of $\text{Ar}^{\text{F}_5}\text{CN}$ from benzimidamido complexes is preceded, having previously been observed in the reactions of insertion complexes **3** and **4** with $\text{Ar}^{\text{F}_5}\text{CN}$.^{7c} The corresponding reactions of the dimethyl, diphenyl, and alkylidene hydrazido analogues of **5** all form stable [2 + 2] cycloaddition products with CS_2 ,^{2v,4g} whereas the imido-derived dithiocarbamates rapidly undergo retrocyclization and formation of isothiocyanates.^{9d}

Reaction of **5** with 1 equiv of $^t\text{BuNCO}$ gave the N,O-bound ureate-type product $\text{Cp}^*\text{Ti}\{\text{PhC}(\text{N}^i\text{Pr})_2\}\{\text{N}(\text{C}\{\text{Ar}^{\text{F}_5}\}\text{NO}^t\text{Bu})\text{C}(\text{N}^t\text{Bu})\text{O}\}$ (**10**; Scheme 3), analogous to **7**, which was isolated as a brown microcrystalline solid in 65% yield upon scale-up. In contrast, reactions with aryl isocyanates (ToINCO and $\text{Ar}'\text{NCO}$ ($\text{Ar}' = 2,6\text{-C}_6\text{H}_3\text{Pr}_2$)) or isothiocyanates ($^t\text{BuNCS}$ and ToINCS) produced complex mixtures and

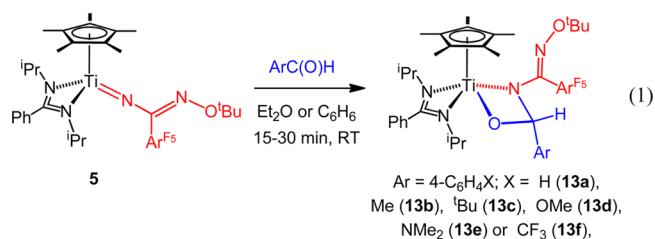
were not investigated further. The NMR data for **10** are consistent with the proposed structure, and the IR spectrum shows a strong band at 1631 cm^{-1} attributed to $\nu(\text{C}=\text{N})$ of the ureate ligand, similar to those found for $\text{Cp}^*\text{Ti}\{\text{MeC}(\text{N}^i\text{Pr})_2\}\{\text{N}(\text{NPh}_2)\text{C}(\text{N}^t\text{Bu})\text{O}\}^{2v}$ and $\text{Cp}^*\text{Ti}\{\text{MeC}(\text{N}^i\text{Pr})_2\}\{\text{N}(\text{Xyl})\text{C}(\text{N}^t\text{Bu})\text{O}\}^{9d}$ (1653 and 1652 cm^{-1} , respectively). Compound **10** is relatively stable in solution at room temperature. Thus, after 16 h, solutions in C_6D_6 undergo less than 10% conversion to the μ -oxo dimer $[\text{Cp}^*\text{Ti}\{\text{PhC}(\text{N}^i\text{Pr})_2\}(\mu\text{-O})_2]$ (**11**)^{7c} and the new imidoilcarbodiimide ${}^t\text{BuNCNC}(\text{Ar}^{\text{F}_5})\text{NO}^t\text{Bu}$ (**12**; Scheme 3), and even after 1 week only ca. 20% conversion occurs. Under analogous conditions, the reaction of $\text{Cp}^*\text{Ti}\{\text{PhC}(\text{N}^i\text{Pr})_2\}(\text{NO}^t\text{Bu})$ (**1**) with ${}^t\text{BuNCO}$ slowly forms the carbodiimide ${}^t\text{BuNCNO}^t\text{Bu}$ and **11** following extrusion from the proposed intermediate $\text{Cp}^*\text{Ti}\{\text{PhC}(\text{N}^i\text{Pr})_2\}\{\text{N}(\text{O}^t\text{Bu})\text{C}(\text{N}^t\text{Bu})\text{O}\}$, which was not observed in this case.^{7c} Therefore, the benzimidamide functional group appears to help stabilize this type of intermediate (i.e., **10**). The behavior of **1** toward ${}^t\text{BuNCO}$ is comparable to that of its imido and dimethyl- and alkylidenehydrazido homologues, whereas the diphenylhydrazide $\text{Cp}^*\text{Ti}\{\text{MeC}(\text{N}^i\text{Pr})_2\}(\text{NNPh}_2)$ forms a $[2 + 2]$ cycloaddition product with ${}^t\text{BuNCO}$ without carbodiimide elimination. DFT studies have shown that both electronic and steric factors are important in such cycloaddition–elimination processes.^{2v,7c,9d}

Heating a solution of **10** to $65\text{ }^\circ\text{C}$ for 15 h nonetheless gave near-quantitative conversion to **12**, along with **11**. Compound **12** was isolated as an analytically pure, yellow oil in 71% yield by distillation ($100\text{ }^\circ\text{C}$, 8×10^{-2} mbar). The ${}^1\text{H}$, ${}^{13}\text{C}$, and ${}^{19}\text{F}$ NMR spectra indicate a single geometric isomer which, by analogy to **13a** (vide infra) and taking into account the steric constraints present in **10**, is assigned as having a *cis* arrangement of the $-\text{O}^t\text{Bu}$ and $-\text{Ar}^{\text{F}_5}$ groups across $({}^t\text{BuO})\text{-N}=\text{C}(\text{Ar}^{\text{F}_5})$ and a *trans* arrangement of groups across $\text{N}=\text{C}=\text{N}$, as shown in Scheme 3. Imidoilcarbodiimides $\text{RNC}(\text{R}^1)\text{-NCNR}^2$ can in general be synthesized from the corresponding imidoilthioureas, $\text{RNC}(\text{R}^1)\text{N}(\text{H})\text{C}(\text{S})\text{NHR}^2$, and have been shown to undergo a rearrangement, forming synthetically useful aminoquinazolines ($\text{R} = \text{Ph}$) or dihydrotriazines ($\text{R} = \text{CHR}'\text{R}''$).¹⁶ The transformation of **5** to **12** shown in Scheme 3 represents a new synthetic method for this type of compound, albeit rather limited in scope and presently without optimization.

Reactions with Benzaldehydes and $\text{HC}(\text{O})\text{NMe}_2$.

Previous reports of the reactions of group 4 imides,^{1b–e,9d,e,17} hydrazides,^{2k,v,4g} and alkoxyimides^{7c} with aldehydes and ketones have shown their tendency to form unstable $[2 + 2]$ cycloaddition products which rapidly extrude the corresponding imine, hydrazone, or oxime ether, respectively. Given the relative stability of **10**, it was hoped that the reaction of **5** with aldehydes and related substrates would likewise form more stable cycloaddition products of the type $\text{Cp}^*\text{Ti}\{\text{PhC}(\text{N}^i\text{Pr})_2\}\{\text{N}(\text{C}\{\text{Ar}^{\text{F}_5}\}\text{NO}^t\text{Bu})\text{C}(\text{R})(\text{R}')\text{O}\}$.

Reactions with Aldehydes. As shown in eq 1, reaction of $\text{PhC}(\text{O})\text{H}$ with **5** rapidly formed the $[2 + 2]$ cycloaddition product $\text{Cp}^*\text{Ti}\{\text{PhC}(\text{N}^i\text{Pr})_2\}\{\text{N}(\text{C}\{\text{Ar}^{\text{F}_5}\}\text{NO}^t\text{Bu})\text{C}(\text{Ph})(\text{H})\text{O}\}$ (**13a**). Compound **13a** formed in quantitative yield on the NMR tube scale and on scale-up was isolated as a dark brown, microcrystalline solid in 82% yield. Only one set of signals were observed in the NMR spectra, consistent with formation of a single diastereomer (both the titanium and PhCH carbon being stereogenic centers). A nuclear Overhauser effect (NOE) experiment showed a through-space interaction between the η -



C_5Me_5 ligand and PhCH of the metallacycle, consistent with the structure shown in eq 1: namely, with the phenyl group oriented away from the $\eta\text{-C}_5\text{Me}_5$ ligand in the sterically least congested arrangement. This geometry was confirmed in the solid state by X-ray diffraction (vide infra). Interestingly, both the PhCH and PhCH signals of **13a** appear as doublets ($J = 2.1$ and 1.4 Hz , respectively) due to $\text{C-H}\cdots\text{F}$ interactions. This is either a consequence of scalar coupling or cross-correlation interactions¹⁸ between PhCH and Ar^{F_5} , as confirmed by a ${}^1\text{H}\{{}^{19}\text{F}\}$ NMR experiment in which PhCH appeared as a singlet. The ${}^{19}\text{F}$ NMR spectrum showed five resonances at room temperature, consistent with restricted rotation about the $\text{C-}C_{\text{ipso}}$ bond to the C_6F_5 ring.

The PhCH “up” arrangement for **13a** is the same as that found in $\text{Cp}^*\text{Ti}\{\text{MeC}(\text{N}^i\text{Pr})_2\}\{\text{N}(\text{N}^t\text{Bu})\text{C}(\text{Ph})(\text{H})\text{O}\}$, formed from $\text{Cp}^*\text{Ti}\{\text{MeC}(\text{N}^i\text{Pr})_2\}(\text{N}^t\text{Bu})$ and $\text{PhC}(\text{O})\text{H}$. In contrast, for the reaction of the homologous tolylimido compound and $\text{PhC}(\text{O})\text{H}$ both isomers were observed,^{9d} as was also the case for the reaction of $\text{Cp}^*\text{Ti}\{\text{PhC}(\text{N}^i\text{Pr})_2\}(\text{NO}^t\text{Bu})$ (**1**) with $\text{PhC}(\text{O})\text{H}$ and $\text{PhC}(\text{O})\text{Me}$.^{7c} Interestingly, whereas **13a** is stable in solution for several hours, all of these previously reported metallacycles rapidly underwent extrusion of the corresponding imines below room temperature, thus preventing their isolation on a preparative scale. To take advantage of this opportunity to study further these types of metallacycles, we prepared a series of homologues; namely, $\text{Cp}^*\text{Ti}\{\text{PhC}(\text{N}^i\text{Pr})_2\}\{\text{N}(\text{C}\{\text{Ar}^{\text{F}_5}\}\text{NO}^t\text{Bu})\text{C}(\text{Ar})(\text{H})\text{O}\}$ ($\text{Ar} = 4\text{-C}_6\text{H}_4\text{X}$; $\text{X} = \text{Me}$ (**13b**), ${}^t\text{Bu}$ (**13c**), OMe (**13d**), NMe_2 (**13e**), CF_3 (**13f**); eq 1). The new compounds were obtained in near-quantitative yields, and their NMR and other data were analogous to those of **13a**, indicating the presence of a single ArCH “up” isomer in each case.

Diffraction-quality crystals of **13a** were grown from a saturated *n*-hexane solution at $4\text{ }^\circ\text{C}$. The molecular structure is shown in Figure 2, and selected distances and angles are given in Table 1. The structure confirms the incorporation of $\text{PhC}(\text{O})\text{H}$ to form a new $\text{N}\{\text{C}(\text{Ar}^{\text{F}_5})\text{NO}^t\text{Bu}\}\text{C}(\text{H})(\text{Ph})\text{O}$ ligand binding to titanium in a $\kappa^2\text{N,O}$ -coordination mode. The stereochemistry around $\text{C}(1)$ is consistent with the solution NOE measurements with $\text{H}(1)$ directed toward the $\eta\text{-C}_5\text{Me}_5$ ligand. The metric parameters associated with both $\text{Cp}^*\text{Ti}\{\text{PhC}(\text{N}^i\text{Pr})_2\}$ and $\text{NC}(\text{Ar}^{\text{F}_5})\text{NO}^t\text{Bu}$ fragments lie within the expected values.¹⁹ The $\text{Ti}(1)\text{-N}(1)$ bond length is increased relative to **5** ($2.0070(16)$ vs $1.747(4)\text{ \AA}$) and is similar to the $\text{Ti-N}_{\text{amidinate}}$ single bonds ($2.1160(18)$ and $2.0972(17)\text{ \AA}$). The $\text{H}(1)\cdots\text{F}(1)$ distance of 2.59 \AA is consistent with the observed doublet coupling in the ${}^1\text{H}$ NMR spectra of **13a–f**. Despite the apparent close proximity of the Ph and Ar^{F_5} rings and the potential for mixed arene–perfluoroarene $\pi\text{-}\pi$ interactions,²⁰ only two close interactions are observed: namely, $\text{C}(2)\cdots\text{C}(9) = 3.054(3)\text{ \AA}$ and $\text{C}(2)\cdots\text{C}(14) = 3.346(3)\text{ \AA}$.

Although the ${}^1\text{H}$ NMR signals for **13a** are not broad at room temperature, spin saturation transfer measurements showed

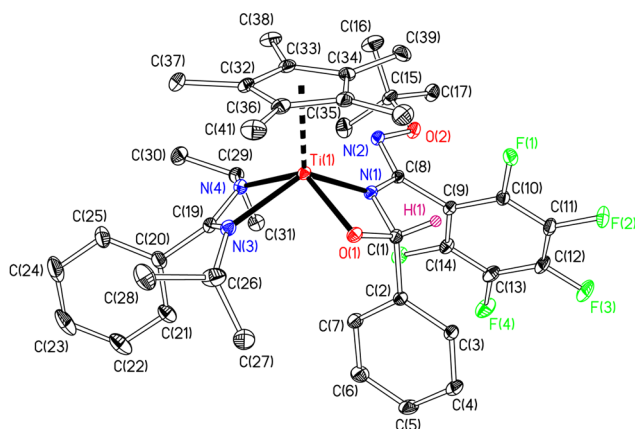


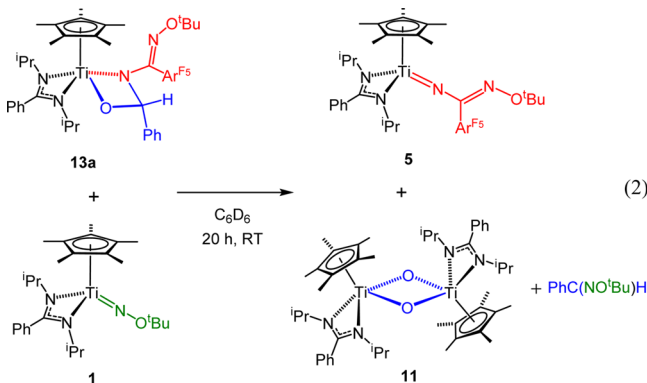
Figure 2. Displacement ellipsoid plot (20% probability) of $\text{Cp}^*\text{Ti}\{\text{PhC}(\text{N}^i\text{Pr})_2\}\{\text{N}(\text{C}\{\text{Ar}^{\text{F}_5}\}\text{NO}^t\text{Bu})\text{C}(\text{Ph})(\text{H})\text{O}\}$ (**13a**). H(1) is drawn as a sphere of an arbitrary radius. All other H atoms are omitted for clarity.

Table 1. Selected Bond Lengths (Å) and Angles (deg) for $\text{Cp}^*\text{Ti}\{\text{PhC}(\text{N}^i\text{Pr})_2\}\{\text{N}(\text{C}\{\text{Ar}^{\text{F}_5}\}\text{NO}^t\text{Bu})\text{C}(\text{Ph})(\text{H})\text{O}\}$ (**13a**)^a

Ti(1)–Cp _{cent}	2.055	N(1)–C(1)	1.469(2)
Ti(1)–N(1)	2.0070(16)	N(1)–C(8)	1.358(2)
Ti(1)–N(3)	2.1160(18)	O(1)–C(1)	1.419(2)
Ti(1)–N(4)	2.0972(17)	C(1)–C(2)	1.519(3)
Ti(1)–O(1)	1.8980(14)		
Cp _{cent} –Ti(1)–N(1)	118.3	Cp _{cent} –Ti(1)–O(1)	118.9
Cp _{cent} –Ti(1)–N(3)	112.6	Cp _{cent} –Ti(1)–N(4)	113.7
N(3)–Ti(1)–N(4)	62.63(7)	O(1)–Ti(1)–N(1)	70.05(6)
Ti(1)–N(1)–C(1)	90.95(11)	Ti(1)–O(1)–C(1)	97.13(10)
O(1)–C(1)–N(1)	101.85(14)		

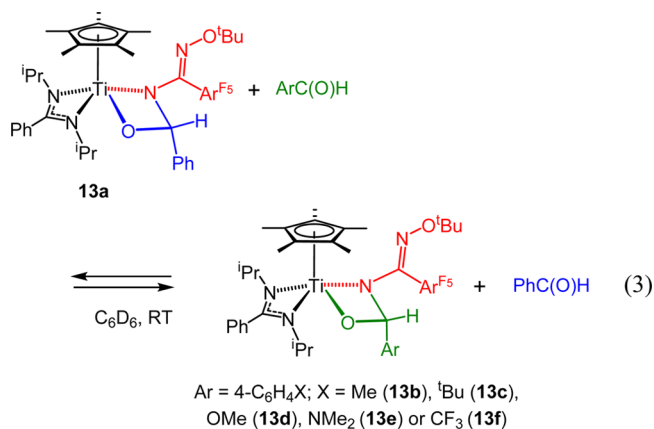
^aCp_{cent} is the computed Cp* ring carbon centroid.

exchange on the NMR time scale between free (added) benzaldehyde and the $\text{PhC}(\text{O})\text{H}$ incorporated in **13a**. This is proposed to occur via a dissociative mechanism, transiently forming **5**, as has been observed previously for related imido compounds and carbonyl complexes.^{9d} As a test of this, bearing in mind the known irreversible reaction of **1** with $\text{PhC}(\text{O})\text{H}$ to form **11** and the oxime ether $\text{PhC}(\text{NO}^t\text{Bu})\text{H}$,^{7c} an NMR tube scale crossover experiment between **13a** and **1** in C_6D_6 was carried out, which showed quantitative formation of the products shown in eq 2.



Previous studies have suggested that electron-withdrawing substituents can help to stabilize metallacyclic complexes

formed from imides (and related systems) and unsaturated substrates.^{2q,s} The relative stability of the complexes $\text{Cp}^*\text{Ti}\{\text{PhC}(\text{N}^i\text{Pr})_2\}\{\text{N}(\text{C}\{\text{Ar}^{\text{F}_5}\}\text{NO}^t\text{Bu})\text{C}(\text{Ar})(\text{H})\text{O}\}$ (**13a–f**) and the reversible addition of $\text{PhC}(\text{O})\text{H}$ to the benzimidamido ligand of **5** prompted us to investigate this further. Thus, ca. 1 equiv of $\text{ArC}(\text{O})\text{H}$ ($\text{Ar} = 4\text{-C}_6\text{H}_4\text{X}$; $\text{X} = \text{Me}, ^t\text{Bu}, \text{OMe}, \text{NMe}_2, \text{CF}_3$) was added to solutions of **13a** in C_6D_6 and the reactions monitored by ^1H NMR spectroscopy (eq 3). Competition equilibria were established within 10 min.



The equilibrium constants (K_{eq}) are given in Table S1 of the Supporting Information and are depicted graphically in semilogarithmic form in Figure 3 against the corresponding

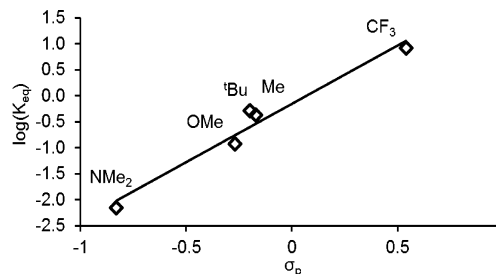
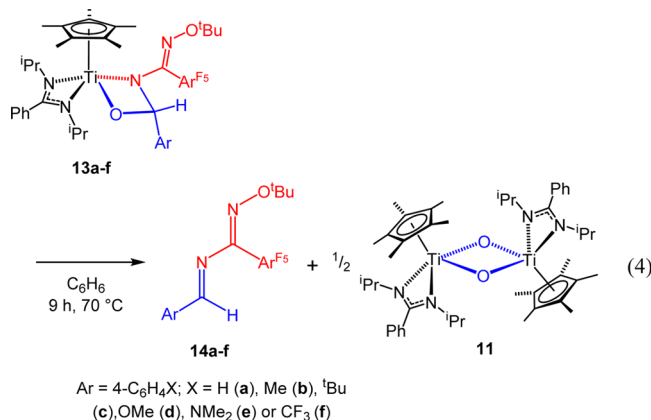


Figure 3. Plot of $\log K_{\text{eq}}$ vs σ_p for the reactions of $\text{Cp}^*\text{Ti}\{\text{PhC}(\text{N}^i\text{Pr})_2\}\{\text{N}(\text{C}\{\text{Ar}^{\text{F}_5}\}\text{NO}^t\text{Bu})\text{C}(\text{Ph})(\text{H})\text{O}\}$ (**13a**) with $\text{ArC}(\text{O})\text{H}$ ($\text{Ar} = 4\text{-C}_6\text{H}_4\text{X}$; $\text{X} = \text{Me}, ^t\text{Bu}, \text{OMe}, \text{NMe}_2, \text{CF}_3$) at 293 K in C_6D_6 . The best-fit line shown has $R^2 = 0.962$.

Hammett substituent constants, σ_p .²¹ The K_{eq} data clearly indicate a thermodynamic preference for cycloaddition products with electron-withdrawing para substituents.

Compound **13a** is not indefinitely stable in solution, and on heating a C_6D_6 solution at 70 °C, a color change from brown to yellow, characteristic of the μ -oxo dimer **11**, is observed. The ^1H NMR spectrum showed quantitative formation of **11** and the 1,3-diazabutadiene derivative $\text{PhC}\{\text{N}(\text{Ar}^{\text{F}_5})\text{NO}^t\text{Bu}\}\text{H}$ (**14a**; eq 4). Analogous results were obtained for **13b–f**, and the corresponding organic products **14a–f** were isolated by sublimation on scale-up in 62–93% yield. Compounds **14a–f** exist predominantly as the single geometric isomer depicted in eq 4 on the basis of the X-ray structure of **14e** and DFT calculations (vide infra). It is interesting to note the *trans* arrangement of the Ar– and $-\text{C}(\text{Ar}^{\text{F}_5})\text{NO}^t\text{Bu}$ groups with respect to the $\text{Ar}(\text{H})\text{C}=\text{N}(\text{Ar}^{\text{F}_5})\text{NO}^t\text{Bu}$ double bond. This is consistent with previous DFT studies of the cycloaddition–extrusion reactions of $\text{Cp}^*\text{Ti}\{\text{PhC}(\text{N}^i\text{Pr})_2\}\{\text{NO}^t\text{Bu}\}$ (**1**) with $\text{PhC}(\text{O})\text{R}$ ($\text{R} = \text{H}, \text{Me}$), in which the metallacycle



intermediates with the PhCR substituent oriented “up” toward Cp* gave rise to the product oxime ether PhC(NO^tBu)R with a *trans* arrangement of the Ph- and -O^tBu groups.^{7c}

The molecular structure of **14e** is shown in Figure S1 of the Supporting Information, and selected bond distances and angles can be found in Table S2. The structure establishes both the connectivity and the geometric isomer isolated. The metric parameters lie within the expected ranges and indicate discrete single and double bonds. The electronic and molecular structure of **14e** and its homologues are discussed in further detail below.¹⁹

The extrusion reaction of Cp*Ti{PhC(NⁱPr)₂}{N(C{Ar^{F5}}-NO^tBu)C(Ph)(H)O} (**13a**) in C₆D₆ was monitored in the temperature range 54–76 °C. The reactions followed first-order kinetics, as judged by linear semilogarithmic plots of ln([**13a**]_t/[**13a**]₀) vs time. An Eyring analysis of the rate constant k_{obs} was carried out (Figure 4), giving the activation

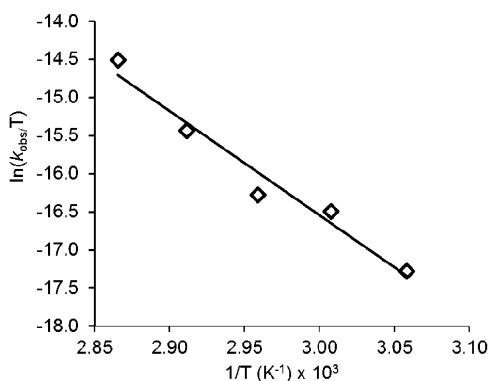


Figure 4. Eyring plot for the extrusion reaction of Cp*Ti{PhC-(NⁱPr)₂}{N(C{Ar^{F5}}-NO^tBu)C(Ph)(H)O} (**13a**) in C₆D₆. Activation parameters are derived from a linear regression analysis ($R^2 = 0.963$): $\Delta H^\ddagger = 27(3)$ kcal mol⁻¹; $\Delta S^\ddagger = 1(9)$ cal mol⁻¹ K⁻¹; $\Delta G_{343}^\ddagger = 27(4)$ kcal mol⁻¹.

parameters $\Delta H^\ddagger = 27(3)$ kcal mol⁻¹ and $\Delta S^\ddagger = 1(9)$ cal mol⁻¹ K⁻¹ ($\Delta G_{343}^\ddagger = 27(4)$ kcal mol⁻¹). The negligible value of ΔS^\ddagger is consistent with an early transition state for these dissociative reactions.²²

The corresponding first-order rate constants (k_{obs}) were also determined for the extrusion reactions of Cp*Ti{PhC(NⁱPr)₂}{N(C{Ar^{F5}}-NO^tBu)C(4-C₆H₄X)(H)O} (X = Me (**13b**), ^tBu (**13c**), OMe (**13d**)) at 70 °C and are given in Table S3 of the Supporting Information, along with representative examples of the corresponding first-order semilogarithmic plots (Figure S2).

The increased k_{obs} values (range [8.09(3)–11.80(8)] × 10⁻⁵ s⁻¹) in comparison to that for **13a** at this temperature (6.79(3) × 10⁻⁵ s⁻¹) show that electron-releasing para substituents reduce the activation energy for extrusion. Attempts to measure k_{obs} at 70 °C for **13e**, possessing the most electron-releasing *p*-NMe₂ substituent, were unsuccessful. The reaction reached greater than 50% completion within 5 min, and the broad ¹H resonances hindered accurate ¹H NMR integration. Therefore k_{obs} for **13e** was measured at 32 °C and the corresponding k_{obs} value for **13a** at 32 °C was calculated from the Eyring plot in Figure 4. Comparison of the k_{obs} values at 32 °C (1.22(1) × 10⁻⁵ s⁻¹ for **13e** vs 0.04 × 10⁻⁵ s⁻¹ for **13a**) shows that extrusion from **13e** is ca. 30 times faster than that from **13a**. The k_{obs} value for **13e** at 70 °C was estimated as 207 × 10⁻⁵ s⁻¹, assuming that $k_{\text{obs}}(70 \text{ °C})/k_{\text{obs}}(32 \text{ °C})$ is the same for both **13a** and **13e** (i.e., that ΔS^\ddagger is negligible in each case, as found experimentally for **13a**, and that the ΔG^\ddagger values for extrusion are primarily controlled by the ΔH^\ddagger terms).

Figure 5 shows a plot of log($k_{\text{obs}}/k_{\text{H}}$) vs σ_p for **13a–e** based on the experimental or estimated k_{obs} values ($k_{\text{H}} = k_{\text{obs}}$ for **13a**;

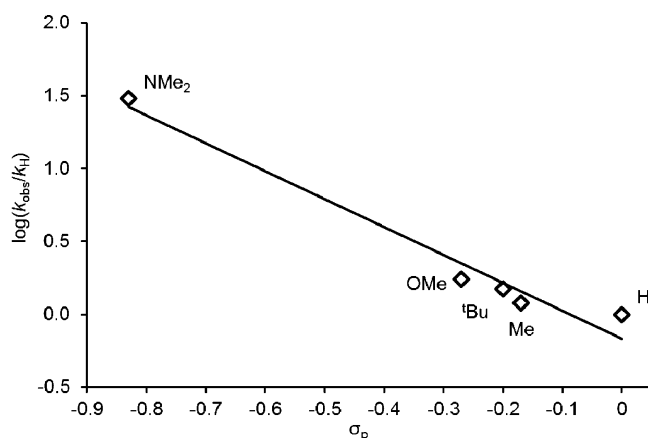
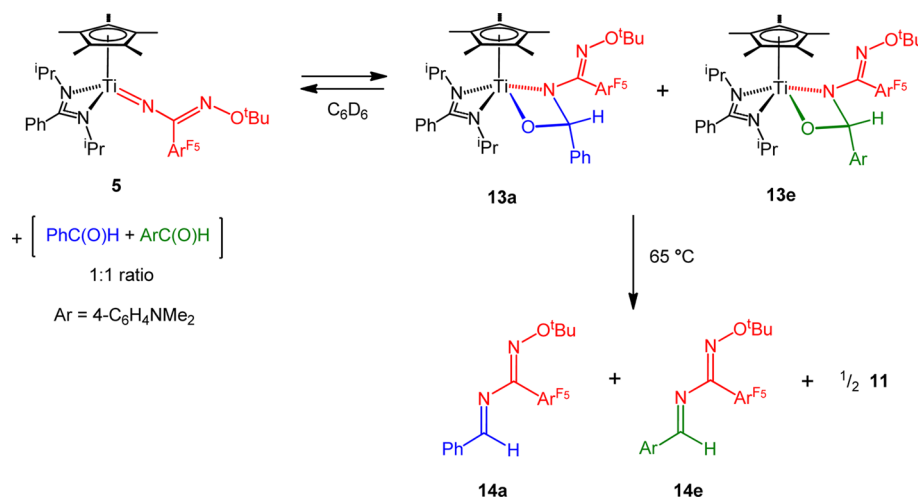


Figure 5. Plot of log($k_{\text{obs}}/k_{\text{H}}$) vs σ_p for the extrusion reaction of Cp*Ti{PhC(NⁱPr)₂}{N(C{Ar^{F5}}-NO^tBu)C(4-C₆H₄X)(H)O} (**13a–e**) at 70 °C in C₆D₆. The best-fit line shown has $R^2 = 0.965$, giving $\rho = -1.9(2)$. k_{H} is k_{obs} for X = H, and k_{obs} for **13e** was estimated from data collected at 32 °C (see Table S3 and Figure S2 (representative individual first-order semilogarithmic plots) of the Supporting Information).

σ_p is the Hammett substituent constant), which gave a reaction constant (ρ) of $-1.9(2)$. This is consistent with a buildup of positive charge on the ArC(H) carbon in the rate-determining step, indicating a transition state consisting more of C–O bond-breaking than of C–N bond-forming character. Unexpectedly, the k_{obs} value of 14.5×10^{-5} s⁻¹ (average of two independent experiments) for compound **13f** was significantly higher than that expected (0.42×10^{-5} s⁻¹) on the basis of the Hammett plot and the data for **13a–e**. We are unable to explain this difference, which may reflect a switch to a different mechanism for this most stable of the metallacycles (cf. the K_{eq} data in Table S1 of the Supporting Information and Figure 3).

Figures 3 and 5 show that, while PhC(O)H forms a more thermodynamically stable metallacycle (**13a**) than (4-C₆H₄NMe₂)C(O)H, the latter (**13e**) is significantly more reactive toward extrusion, forming **14e**. Scheme 4 summarizes a competition experiment that illustrates this interplay. Addition of an equimolar solution of PhC(O)H and (4-C₆H₄NMe₂)C(O)H to **5** (1:1:1 initial ratio) in C₆D₆ at room temperature

Scheme 4. Reaction of $\text{Cp}^*\text{Ti}\{\text{PhC}(\text{N}^i\text{Pr})_2\}\{\text{NC}(\text{Ar}^{\text{F}_5})\text{NO}^t\text{Bu}\}$ (**5**) with $\text{PhC}(\text{O})\text{H}$ and $\text{ArC}(\text{O})\text{H}$ ($\text{Ar} = 4\text{-C}_6\text{H}_4\text{NMe}_2$; 1:1 Ratio)^a



^a13a and 13e are formed in a 10:1 ratio and 14a and 14e in a 2:1 ratio.

gave predominantly **13a** and unreacted $(4\text{-C}_6\text{H}_4\text{NMe}_2)\text{C}(\text{O})\text{H}$ (**13a:13e** \approx 10:1 in accordance with Figure 3). After the mixture was heated to 65 °C for 21 h, the ¹H NMR spectrum showed formation of the organic products **14a,e** in a ca. 2:1 ratio, in accordance with the Curtin–Hammett principle.²³

The organic products **14a–d** were isolated as white/cream solids, and **14f** was a pale yellow oil. In contrast, **14e** was obtained as an orange solid, suggesting a significant effect of the *p*-NMe₂ group on the electronic structure. Table 2 gives the

Table 2. Experimental λ_{max} Values (nm) and Absorption Coefficients (ϵ) for $(4\text{-C}_6\text{H}_4\text{X})\text{C}\{\text{NC}(\text{Ar}^{\text{F}_5})\text{NO}^t\text{Bu}\}\text{H}$ (**14a–f**), Together with HOMO–LUMO Gaps (eV) Determined by DFT^a

compound	<i>p</i> -X	λ_{max} (nm)	$\epsilon \times 10^{-4}$ (M ⁻¹ cm ⁻¹)	HOMO–LUMO separation (eV)
14a	H	271	3.0	2.64
14b	Me	275	5.4	2.60
14c	^t Bu	275	3.7	2.61
14d	OMe	281	5.8	2.53
14e	NMe ₂	360	5.3	2.28
14f	CF ₃	274	1.4	2.55

^aThe spectra were measured as *n*-hexane solutions.

experimental λ_{max} values and absorption coefficients for the lowest energy bands in the UV–visible spectra of **14a–f** measured in *n*-hexane. The absorption coefficients lie in the range $(1.4\text{--}5.8) \times 10^4 \text{ M}^{-1} \text{ cm}^{-1}$ and do not vary in a systematic manner. However, whereas the λ_{max} values for **14a–d,f** appear between ca. 271 and 281 nm, that for **14e** is at 360 nm, tailing into the blue end of the visible spectrum, accounting for the orange color. UV–visible spectra were also measured for **14a,e** in MeOH, the higher dielectric constant ($\epsilon = 32.6$)²⁴ resulting in a small bathochromic shift in the λ_{max} value in each case ($\Delta\lambda_{\text{max}} = 15$ and 23 nm, respectively) but having no significant effect on the extinction coefficients.

DFT calculations were carried out at the GGA:BP/TZP level on minimized geometries of compounds **14a–f** and, as expected, revealed generally similar electronic structures. Figure 6 depicts isosurfaces for the HOMO and LUMO of **14a,e**;

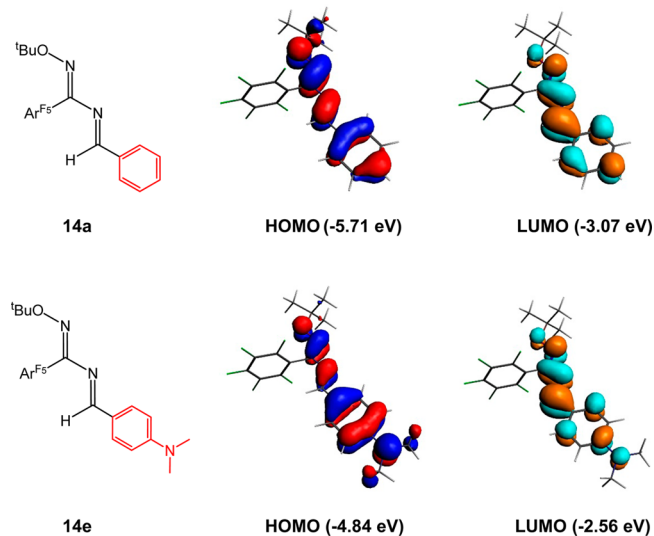
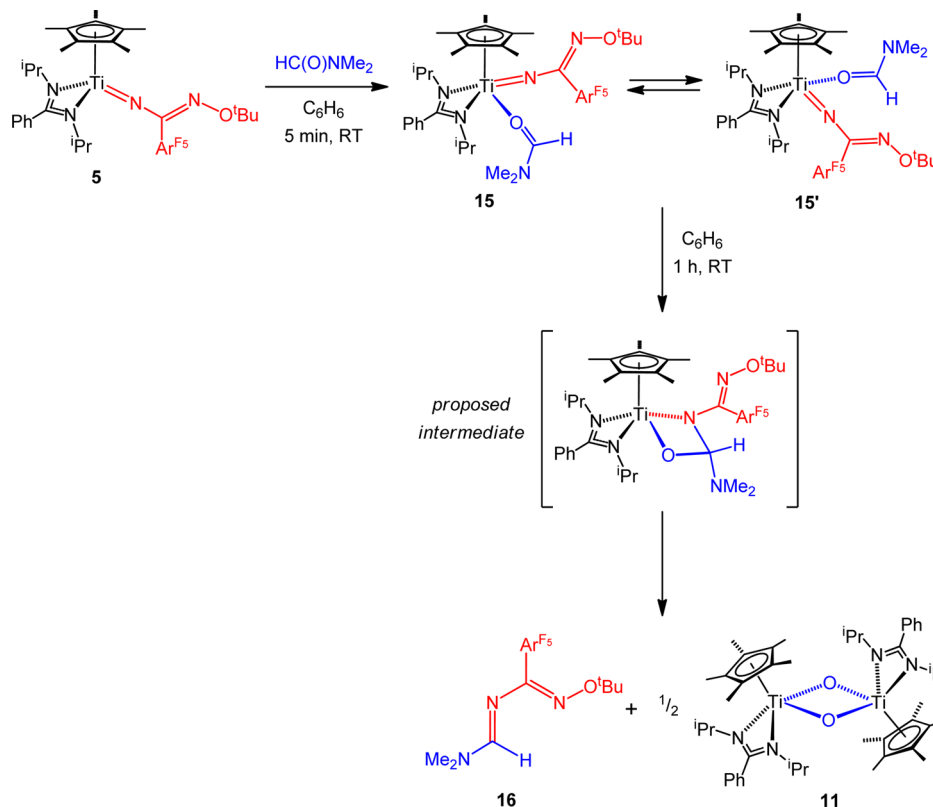


Figure 6. Isosurfaces and energies of the HOMO and LUMO of $\text{PhC}\{\text{NC}(\text{Ar}^{\text{F}_5})\text{NO}^t\text{Bu}\}\text{H}$ (**14a**, top) and $(4\text{-C}_6\text{H}_4\text{NMe}_2)\text{C}\{\text{NC}(\text{Ar}^{\text{F}_5})\text{NO}^t\text{Bu}\}\text{H}$ (**14e**, bottom).

further details for the other derivatives are given in Figure S3 of the Supporting Information. The computed HOMO–LUMO separations are given for all of the compounds in Table 2. For **14a–d,f** the values fall in the range 2.53–2.64 eV. For **14e** the value is 2.28 eV and hence the trends in HOMO–LUMO separations qualitatively correspond well with the trends in λ_{max} .²⁵ The destabilizing effect of the *p*-NMe₂ substituent on both the HOMO and LUMO of **14e** is evident from Figure 6 (bottom), which clearly shows the antibonding aryl(π)–NMe₂($2p_\pi$) interaction in each orbital. This is responsible for the general destabilization of these frontier MOs relative to those of **14a** (Figure 6, top). However, while the HOMO of **14e** is destabilized by 0.87 eV, the LUMO is only destabilized by 0.51 eV, explaining the decrease in HOMO–LUMO separation from **14a** to **14e**. Mulliken population analyses found that the NMe₂($2p_\pi$) atomic orbital contributions to the HOMO and LUMO of **14e** are 18% and 3.4%, respectively, consistent with the different changes in energy. Similarly, the

Scheme 5. Reaction of $\text{Cp}^*\text{Ti}\{\text{PhC}(\text{N}^i\text{Pr})_2\}\{\text{NC}(\text{Ar}^{\text{F}_5})\text{NO}^t\text{Bu}\}$ (**5**) with $\text{HC}(\text{O})\text{NMe}_2$ 

next smallest HOMO–LUMO separation (and next longest λ_{max}) was found for **14d** (*p*-OMe group), although the higher electronegativity of oxygen in comparison with nitrogen leads to an overall decrease in contribution of the OMe($2p_{\pi}$) lone pair to both the HOMO and LUMO (8.6% and 2.2% contributions, respectively).

Reactions with Ketones and $\text{HC}(\text{O})\text{NMe}_2$. Reaction of **5** with either PhC(O)Me or PhC(O)Ph gave disappointing results. The reaction with PhC(O)Me in C₆D₆ at room temperature generated a complex mixture of products within 15 min.^{9d} Analogous results were found for $\text{Cp}^*\text{Ti}\{\text{MeC}(\text{N}^i\text{Pr})_2\}$ -(NTol) with ketones of the type RC(O)Me, and it was proposed that concomitant side reactions stemming from the enol tautomers (RC(OH)CH₂) may be responsible.²⁶ Heating to 70 °C was required to effect a reaction between **5** and PhC(O)Ph, and even after 9 days it had only reached ca. 45% conversion. At this point the ¹H NMR spectrum also showed significant impurities and was not investigated further. In contrast, reaction between **5** and $\text{HC}(\text{O})\text{NMe}_2$ in C₆D₆ formed the fluxional intermediate $\text{Cp}^*\text{Ti}\{\text{PhC}(\text{N}^i\text{Pr})_2\}\{\text{NC}(\text{Ar}^{\text{F}_5})\text{NO}^t\text{Bu}\}\{\text{OC}(\text{NMe}_2)\text{H}\}$ (**15**) within 5 min. This, in turn, converted quantitatively to the μ -oxo dimer **11** and the 1,3-diazabutadiene $\text{Me}_2\text{N}\{\text{NC}(\text{Ar}^{\text{F}_5})\text{NO}^t\text{Bu}\}\text{H}$ (**16**) after 1 h (Scheme 5; 10% conversion after 5 min). On scale-up **16** was isolated by sublimation as a white solid in 64% yield and its identity confirmed by X-ray diffraction (vide infra).

Compound **15** was too unstable to be isolated, and the resonances of the Cp*, PhC(N^{*i*}Pr)₂, and HC(O)NMe₂ group were only slightly shifted from those of **5** and the free formamide. Accordingly, by analogy to the crystallographically characterized σ adduct $\text{Cp}^*\text{Ti}\{\text{PhC}(\text{N}^i\text{Pr})_2\}\{\text{NC}(\text{Ar}^{\text{F}_5})\text{NO}^t\text{Bu}\}\{\text{CN}^t\text{Bu}\}$ (**18**; vide infra) it was assigned the structure shown in Scheme 5, existing in dynamic equilibrium on the

NMR timescale with the enantiomer **15'**, as implied by the apparent molecular C_s symmetry. Compound **16** is proposed to form by a cycloaddition–extrusion mechanism similar to that established for **14a–f**. The fast reaction and lack of observation of any intermediates (i.e., analogues of **13a–f**) are consistent with the strong π -donor ability of the –NMe₂ group which, by analogy with the results for the reactions with ArC(O)H, would both destabilize any intermediate metallacycle and accelerate the rate of extrusion of **16** from it.

The solid-state structures of $(4\text{-C}_6\text{H}_4\text{NMe}_2)\text{C}\{\text{NC}(\text{Ar}^{\text{F}_5})\text{NO}^t\text{Bu}\}\text{H}$ (**14e**) and **16** are shown in Figure S1 and selected bond distances and angles are given in Tables S2 and S4 of the Supporting Information. In general terms the metric parameters lie within the expected ranges for the various bond types and functional groups.^{19,27} In particular, the N(1)–C(5) and N(2)–C(12) distances (range 1.281(5)–1.2990(16) Å) and N(2)–C(5) distances (1.394(5) and 1.3826(15) Å) are consistent with double and single bonds and the 1,3-diazabutadiene structures shown in eq 4 and Scheme 5. The Ar^{F5} ring is approximately orthogonal to the N(1)–C(5)–N(2) moiety in each compound (angles between the least-squares planes of 76.8 and 68.8°), whereas the –C₆H₄NMe₂ and –NMe₂ groups are approximately coplanar with the C(12)–N(2)–C(5) linkage, as shown by the dihedral angles N(2)–C(12)–C(13)–C(14,18) = 3.1° (average) and N(2)–C(12)–N(3)–C(13,14) = 3.9° (average). The most significant difference between **14e** and **16** is the geometry about the N(2)–C(5) bond. Compound **14e** adopts a *transoid* conformation of the C=N double bonds, whereas **16** has a *cisoid* form (cf. Figure 7), as quantified by the N(1)–C(5)–N(2)–C(12) dihedral angles of 174.8 and 35.3°, respectively. For **14e** this dihedral angle is close to the ideal value of 180°, whereas for **16** it deviates significantly from 0° due to repulsion

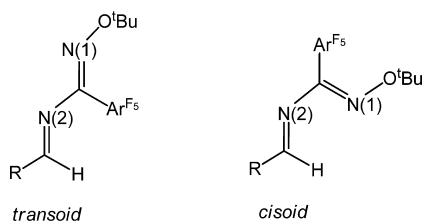


Figure 7. *transoid* and *cisoid* isomers of $\text{RC}\{\text{NC}(\text{Ar}^{\text{F}_5})\text{NO}^t\text{Bu}\}\text{H}$ ($\text{R} = 4\text{-C}_6\text{H}_4\text{X}$ (**14a–f**), NMe_2 (**16**), H (**17**)).

between H(1) and the N(1) lone pair. The relatively poor precision of the structure for **14e** (due to the poorly diffracting nature of the crystals) prevents a more detailed comparison of its individual bond distances and angles with those of **16**, but analysis of the DFT computed structures for each compound confirmed the general structural features.

To explore further these differences in apparent conformational preference, DFT calculations were carried out on $\text{PhC}\{\text{NC}(\text{Ar}^{\text{F}_5})\text{NO}^t\text{Bu}\}\text{H}$ (**14a**), **14e**, and **16** in their *transoid* and *cisoid* conformations. Corresponding calculations were also carried out on the hypothetical $\text{HC}\{\text{NC}(\text{Ar}^{\text{F}_5})\text{NO}^t\text{Bu}\}\text{H}$ (**17**) with H in place of the $4\text{-C}_6\text{H}_4\text{X}$ or NMe_2 groups of **14a,e** and **16**. In each case the calculated geometries and metric parameters compared well with the experimental values: namely, a well-defined 1,3-diazabutadiene structure with an approximately coplanar $-\text{N}(1)=\text{C}-\text{N}(2)=\text{C}-$ linkage in the *transoid* conformations and a somewhat twisted arrangement for the *cisoid* forms. Since the calculations found no significant or systematic difference in entropy between each pair of conformers (ΔS typically varied between ca. -0.5 and 1.5 $\text{cal mol}^{-1} \text{K}^{-1}$), we focus only on the differences in enthalpy (ΔH).²⁸

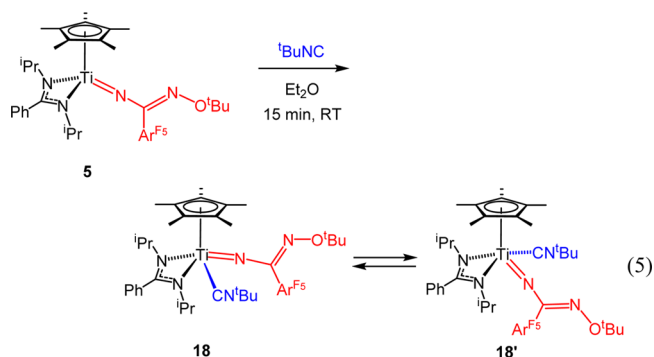
In agreement with the experimental structures, the *transoid* isomer of **14e** was 0.67 kcal mol^{-1} more stable than the *cisoid* alternative, whereas for **16** the *cisoid* conformer was the more stable isomer by a similar amount ($\Delta H = 0.65$ kcal mol^{-1}). The enthalpy difference ($\Delta H = 0.80$ kcal mol^{-1}) in favor of the *transoid* form for **14a** was slightly larger than for **14e**, suggesting that the *p*- NMe_2 group in the latter slightly destabilizes the *transoid* conformer relative to the *cisoid* form. For the hypothetical $\text{HC}\{\text{NC}(\text{Ar}^{\text{F}_5})\text{NO}^t\text{Bu}\}\text{H}$ (**17**), having only a H atom in place of $4\text{-C}_6\text{H}_4\text{X}$ or NMe_2 , the *transoid* form was 1.23 kcal mol^{-1} more stable, showing that this is the intrinsically more stable conformer in this type of system, although the energy differences are all rather small. Examination of the Mulliken atomic charges (q) for N(2) revealed that changing the R group in *transoid*- $\text{RC}\{\text{NC}(\text{Ar}^{\text{F}_5})\text{NO}^t\text{Bu}\}\text{H}$ from H to progressively better π -donor substituents gave a build-up of charge on this atom: $\text{R} = \text{H}$, $q(\text{N}(2)) = -0.2291$; $\text{R} = \text{Ph}$, $q(\text{N}(2)) = -0.2578$; $\text{R} = 4\text{-C}_6\text{H}_4\text{NMe}_2$, $q(\text{N}(2)) = -0.2751$; $\text{R} = \text{NMe}_2$, $q(\text{N}(2)) = -0.3286$. Therefore, it seems that increased lone pair repulsion between N(2) and N(1) in the *transoid* conformer with increasing R group π donation may be an important factor leading to a switch toward the *cisoid* alternative.

The small ΔH values suggest that both the *transoid* and *cisoid* forms of **14a–f** and **16** may exist in solution, since ΔH values of ca. ± 0.70 kcal mol^{-1} (assuming $\Delta S \approx 0$ as discussed) correspond to ca. 1:(± 4) ratios of conformers. Although only one set of NMR resonances is seen experimentally in all cases, we considered it possible that both conformers could be

present in solution but be in fast dynamic equilibrium on the NMR time scale. To determine whether *cisoid* \leftrightarrow *transoid* interconversions might be energetically feasible, the corresponding transition states were determined by DFT for the *transoid* to *cisoid* isomerization of **14a,e** ($\Delta H^\ddagger = 4.71$ and 4.36 kcal mol^{-1} , respectively) and for the *cisoid* to *transoid* isomerization of **16** ($\Delta H^\ddagger = 3.78$ kcal mol^{-1}). The computed ΔS^\ddagger values were small and were in the range -3 to -5 $\text{cal mol}^{-1} \text{K}^{-1}$. Taken together, the DFT calculations estimate that the maximum ΔG^\ddagger value for the *cisoid* \leftrightarrow *transoid* transformations is less than ca. 6.5 kcal mol^{-1} at 298 K. This readily accessible barrier is consistent with the observation of a single time-averaged set of NMR resonances in all cases.

Reactions with Isonitriles. There have been a number of reports of the reactions of transition-metal imido and hydrazido complexes with organic isonitriles, with the commercially available $^t\text{BuNC}$ and XylNC derivatives being the most commonly studied.^{1a,b,e} $[1 + 2]$ addition of RNC to the $\text{M}=\text{NR}'$ bond of imides or hydrazides forms η^2 -carbodiimide complexes of the type $(\text{L})\text{M}(\eta^2\text{-RNCNR}')$, which have been isolated in several cases for $\text{R}' = \text{hydrocarbyl}$.^{15,29} In other instances the first-formed carbodiimides are not observed but undergo further reactions. These include reactions with further equivalent(s) of isonitrile, giving new heterocyclic complexes,³⁰ or in the case of certain group 4 diphenylhydrazido complexes, $\text{N}_\alpha\text{-N}_\beta$ bond cleavage resulting in mixed amide-metalated carbodiimide complexes $(\text{L})\text{M}(\text{NPh}_2)(\text{NCNR})$.^{2s,z,3b} In some instances, reaction with the $\text{M}=\text{NR}'$ bond does not occur and RNC σ adducts can be isolated.^{4g,31} We have previously reported on the reactions of $\text{Cp}^*\text{Ti}\{\text{RC}(\text{N}^i\text{Pr})_2\}(\text{NR}')$ ($\text{R} = \text{Me}, \text{Ph}$; $\text{R}' = ^t\text{Bu}, \text{aryl}, \text{NPh}_2, \text{NMe}_2, \text{NNCPh}_2, \text{O}^t\text{Bu}$ (**1**)) with isonitriles. In the case of the imido complexes no reaction was observed, whereas unknown mixtures were formed with the diphenylhydrazido compound or **1**.^{7c,31c} The other complexes formed labile σ adducts, one of which was structurally characterized.^{4g,31c}

Reaction of **5** with $^t\text{BuNC}$ in Et_2O at room temperature formed the σ adduct $\text{Cp}^*\text{Ti}\{\text{PhC}(\text{N}^i\text{Pr})_2\}\{\text{NC}(\text{Ar}^{\text{F}_5})\text{NO}^t\text{Bu}\}(\text{CN}^t\text{Bu})$ (**18**, eq 5), which was isolated in 61% yield after



crystallization from pentane. When the reaction was followed on the NMR tube scale in C_6D_6 , the conversion was quantitative. The NMR spectrum at room temperature indicated a C_s -symmetric product on the NMR time scale. This is attributed to the rapid interconversion between the two enantiomers **18** and **18'** (eq 5). Cooling a solution of **18** in toluene- d_8 showed the isopropyl groups as two apparent septets and four doublets, although the resonances remained broad, even at -80 $^\circ\text{C}$. At this temperature the *o*- and *m*- C_6F_5 ^{19}F resonances were inequivalent, indicative of restricted rotation

about the N_2C-C_{ipso} bond of the benzimidamido ligand. The IR spectrum of **18** shows a strong $\nu(C\equiv N)$ band at 2186 cm^{-1} , at a frequency higher than that for free $t\text{BuNC}$ (2138 cm^{-1}), consistent with coordination to the electron-deficient titanium.³² The $\nu(C\equiv N)$ band is at a higher frequency than those for $\text{Cp}^*\text{Ti}\{\text{MeC}(\text{N}^i\text{Pr})_2\}(\text{NNCPh}_2)(\text{CN}^t\text{Bu})$ (2164 cm^{-1})⁴⁸ and the comparatively labile σ adduct $\text{Cp}^*\text{Ti}\{\text{MeC}(\text{N}^i\text{Pr})_2\}(\text{NNMe}_2)(\text{CN}^t\text{Bu})$ ^{31c} (2152 cm^{-1}). Other examples of titanium d^0 *tert*-butyl isocyanide adducts include (MPB)- $\text{TiCl}_2(\text{CN}^t\text{Bu})$ (MPB²⁻ = 2,2'-methylenebis(6-*tert*-butyl-4-methylphenolate) dianion)³³ and $\text{TiCl}_4(\text{CN}^t\text{Bu})_2$.^{32b}

Diffraction-quality crystals of **18** were grown from a saturated pentane solution at $-30\text{ }^\circ\text{C}$. The molecular structure is shown in Figure 8, and selected distances and angles are given in Table

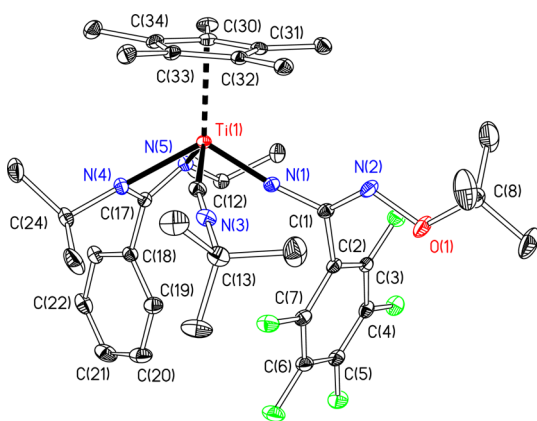


Figure 8. Displacement ellipsoid plot (20% probability) of $\text{Cp}^*\text{Ti}\{\text{PhC}(\text{N}^i\text{Pr})_2\}\{\text{NC}(\text{Ar}^{\text{F}_5})\text{NO}^t\text{Bu}\}(\text{CN}^t\text{Bu})$ (**18**). H atoms are omitted for clarity.

Table 3. Selected Bond Lengths (Å) and Angles (deg) for $\text{Cp}^*\text{Ti}\{\text{PhC}(\text{N}^i\text{Pr})_2\}\{\text{NC}(\text{Ar}^{\text{F}_5})\text{NO}^t\text{Bu}\}(\text{CN}^t\text{Bu})$ (**18**)^a

Ti(1)–Cp _{cent}	2.091	Ti(1)–C(12)	2.191(2)
Ti(1)–N(1)	1.7739(17)	N(3)–C(12)	1.153(3)
Ti(1)–N(4)	2.1459(17)	N(3)–C(13)	1.462(3)
Ti(1)–N(5)	2.1957(17)		
Cp _{cent} –Ti(1)–N(1)	119.37	Cp _{cent} –Ti(1)–N(5)	115.62
Cp _{cent} –Ti(1)–N(4)	121.35	Cp _{cent} –Ti(1)–C(12)	104.69
N(4)–Ti(1)–N(5)	62.09(6)	Ti(1)–C(12)–N(3)	167.35(19)
Ti(1)–N(1)–C(1)	169.81(15)	C(12)–N(3)–C(13)	179.5(2)

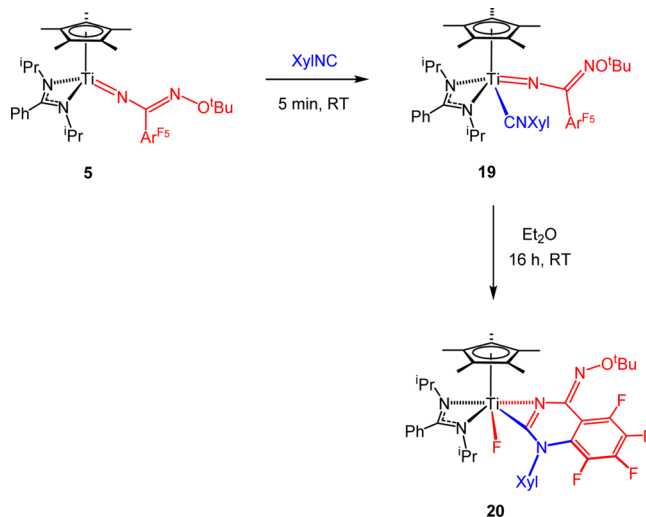
^aCp_{cent} is the computed Cp* ring carbon centroid.

3. The structure confirms **18** as a half-sandwich complex with a four-legged piano-stool geometry around the metal with η^5 -C₅Me₅ and κ^2N,N' -amidinate ligands and is similar to that reported recently for $\text{Cp}^*\text{Ti}\{\text{MeC}(\text{N}^i\text{Pr})_2\}(\text{NNCPh}_2)(\text{CNXyl})$.⁴⁸ The Ti(1)–C(12) bond distance of 2.191(2) Å in **18** is relatively short in comparison to those of other titanium(+4) isocyanide adducts (2.232(2)–2.256(6) Å), consistent with the relatively high frequency observed for $\nu(C\equiv N)$.^{48,32b–d} The σ -only nature of the Ti–CN^tBu bond is also indicated by the short C(12)–N(3) bond distance of 1.153(3) Å. The Ti(1)–N(1) bond is slightly longer than that in **5** (1.7739(17) in **18** vs 1.747(4) Å), which is attributed to the increased coordination number around titanium.

No further reaction was found for **18** at room temperature, and after 18 h at 70 °C in C₆D₆ only new low-intensity resonances were observed. After 5 days complicated mixtures were formed and this reaction was not scaled up. The poor reactivity of **18** is probably due to the steric demands of the ^tBuNC ligand.

Reaction of **5** with XylNC on the NMR tube scale in C₆D₆ resulted in the immediate and quantitative formation of $\text{Cp}^*\text{Ti}\{\text{PhC}(\text{N}^i\text{Pr})_2\}\{\text{NC}(\text{Ar}^{\text{F}_5})\text{NO}^t\text{Bu}\}(\text{CNXyl})$ (**19**; Scheme 6), which is unstable at room temperature and was

Scheme 6. Reaction of $\text{Cp}^*\text{Ti}\{\text{PhC}(\text{N}^i\text{Pr})_2\}\{\text{NC}(\text{Ar}^{\text{F}_5})\text{NO}^t\text{Bu}\}$ (**5**) with XylNC



characterized in situ. The dynamic NMR behavior is analogous to that for **18**: the room-temperature NMR spectra indicate a C₅-symmetric compound, while at $-70\text{ }^\circ\text{C}$ the resonances are reminiscent of those for **18**. Over a period of ca. 16 h **19** converted quantitatively to a new compound, $\text{Cp}^*\text{Ti}\{\text{PhC}(\text{N}^i\text{Pr})_2\}\{\text{NC}(\text{NO}^t\text{Bu})\text{C}_6\text{F}_4\text{N}(\text{Xyl})\text{C}\}(\text{F})$ (**20**), which was isolated as an orange powder in 85% yield after scale-up in diethyl ether. Diffraction-quality crystals were grown from *n*-hexane. The molecular structure is shown in Figure 9, and selected bond distances and angles are given in Table 4.

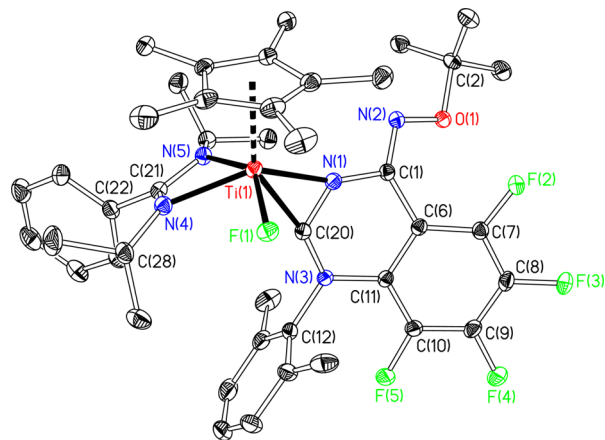


Figure 9. Displacement ellipsoid plot (20% probability) of $\text{Cp}^*\text{Ti}\{\text{PhC}(\text{N}^i\text{Pr})_2\}\{\text{NC}(\text{NO}^t\text{Bu})\text{C}_6\text{F}_4\text{N}(\text{Xyl})\text{C}\}(\text{F})$ (**20**). H atoms are omitted for clarity.

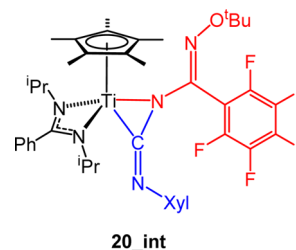
Table 4. Selected Bond Lengths (Å) and Angles (deg) for $\text{Cp}^*\text{Ti}\{\text{PhC}(\text{N}^i\text{Pr})_2\}\{\text{NC}(\text{NO}^t\text{Bu})\text{C}_6\text{F}_4\text{N}(\text{Xyl})\text{C}\}(\text{F})$ (Xyl = 2,6- $\text{C}_6\text{H}_3\text{Me}_2$, 20)

Ti(1)–Cp _{cent}	2.115	N(1)–C(1)	1.414(2)
Ti(1)–C(20)	2.1407(18)	N(2)–C(1)	1.283(2)
Ti(1)–N(1)	2.0773(16)	N(3)–C(11)	1.417(2)
Ti(1)–N(4)	2.1089(17)	N(3)–C(12)	1.456(2)
Ti(1)–N(5)	2.2471(16)	N(3)–C(20)	1.367(2)
Ti(1)–F(1)	1.8688(11)	C(6)–C(1)	1.472(3)
N(1)–C(20)	1.305(2)	C(11)–C(6)	1.416(3)
Cp _{cent} –Ti(1)–N(1)	113.3	Cp _{cent} –Ti(1)–N(5)	109.23
Cp _{cent} –Ti(1)–N(4)	110.17	Cp _{cent} –Ti(1)–C(20)	148.90
Cp _{cent} –Ti(1)–F(1)	101.81	N(4)–Ti(1)–N(5)	60.31(6)
Ti(1)–N(1)–C(20)	74.65(10)	Ti(1)–C(20)–N(1)	69.35(10)
C(1)–N(2)–O(1)	111.76(15)	N(1)–C(1)–N(2)	116.64(16)

Compound **20** is a half-sandwich complex with a five-legged piano-stool geometry. In addition to the expected $\eta^5\text{-C}_5\text{Me}_5$ and $k^2\text{N,N'}$ -amidinate ligands, the titanium is coordinated to a fluoride ligand and a new heterocyclic fragment derived from the XylNC (i.e., C(20), N(3), and the xyl group) and benzimidamido ligands of **19**. The metric parameters for the $\text{Cp}^*\text{Ti}\{\text{PhC}(\text{N}^i\text{Pr})_2\}$ fragment lie within the expected values and are similar to those for complexes supported by this ligand set. The Ti(1)–F(1) bond length of 1.8688(11) Å lies within the range reported for other cyclopentadienyl-supported titanium complexes reported in the literature (range 1.812–1.937 Å).¹⁹ The heterocyclic fragment may be viewed as a 2-metallated 1-arylquinazolin-4(1H)-one oxime ether. The Ti(1)–N(1) and Ti(1)–C(20) bond distances of 2.0773(16) and 2.1407(18) Å, respectively, are consistent with this description. The C(20)–N(1) and C(1)–N(2) bond lengths are indicative of C=N double bonds (1.305(2) and 1.283(2) Å, respectively). The intermediate distances for N(3)–C(20) (1.367(2) Å) and N(1)–C(1) (1.414(2) Å) indicate slightly differing extents of delocalization. The NMR data are consistent with this C_1 -symmetric complex existing also in solution. In particular, one singlet and four multiplets were observed in the ¹⁹F NMR spectrum at –20 °C, the singlet being at δ –101.8 ppm, which suggested that it may no longer be bonded to carbon. A ¹⁹F COSY NMR experiment showed scalar coupling between the other four ¹⁹F atoms (range δ –118.7 to –162.7 ppm) but no apparent coupling to the singlet resonance. In the ¹³C NMR spectrum the quaternary signal corresponding to the metal-bound C(20) was observed at δ 216.7 ppm.

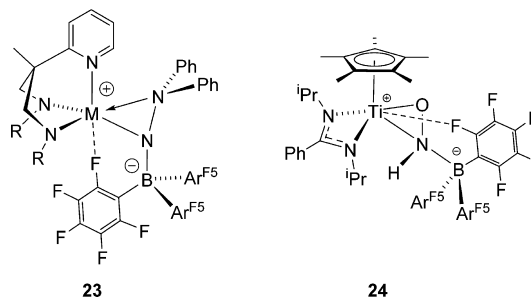
Following the initial formation of **19**, the mechanism for formation of **20** is proposed to proceed via [1 + 2] addition of XylNC to $\text{Ti}=\text{NC}(\text{Ar}^{\text{F}_5})\text{NO}^t\text{Bu}$, forming **20_int** containing an η^2 -carbodiimide ligand. Related compounds have been reported previously: for example, in the reactions of $\text{Cp}^*\text{Ir}(\text{N}^t\text{Bu})$ ¹⁵ and $\text{Cp}_2\text{Zr}(\text{N}^t\text{Bu})(\text{THF})$ ²⁹ with ^tBuNC. Subsequent nucleophilic attack by XylNC on the ortho position of the Ar^{F_5} group displaces the fluorine, which forms a new bond to titanium. Other examples of C–F activation using d^0 group 4 metal species have been reported,³⁴ and titanium fluoride compounds are not uncommon.^{34,35} Quinazoline-type compounds have been used in the synthesis of many pharmaceutical agents, including antifungal, anticancer, and anti-HIV drugs.³⁶ Conventional synthetic routes to quinazolines include reaction of 2-aminobenzophenones and benzylic amines in the presence of I_2 and *tert*-butyl hydroperoxide,³⁷ using (2-bromophenyl)-

methylamines with amides in the presence of air, CuI, K_2CO_3 , and *i*-PrOH,³⁸ and using imidoilcarbodiimides.¹⁶



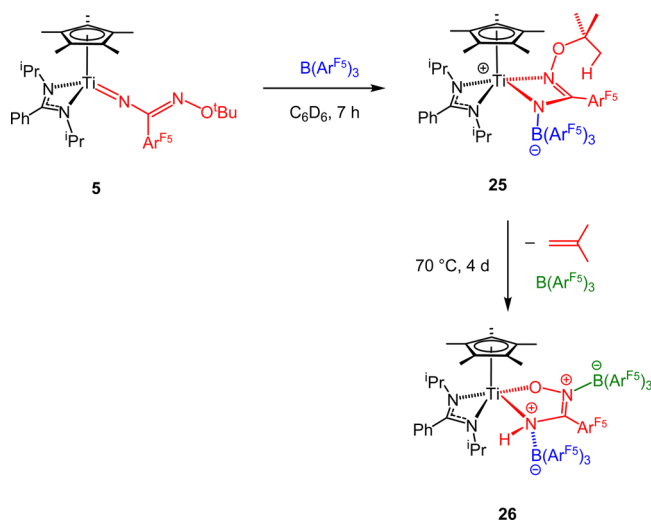
In an attempt to extend this reactivity, XylNC was added to a C_6D_6 solution of $\text{Cp}^*\text{Ti}\{\text{PhC}(\text{N}^i\text{Pr})_2\}\{\text{NC}(\text{Ar}^{\text{F}_5})\text{NO}^t\text{Bu}\}$ (**4**) and the reaction monitored by ¹H and ¹⁹F NMR spectroscopy. Within 5 min a σ adduct, $\text{Cp}^*\text{Ti}\{\text{PhC}(\text{N}^i\text{Pr})_2\}\{\text{NC}(\text{Ar}^{\text{F}_5})\text{NO}^t\text{Bu}\}(\text{CNXyl})$ (**21**), analogous to **18** and **19** was formed and characterized by NMR in situ. After 16 h at room temperature a second set of signals were observed in the ¹H and ¹⁹F NMR spectra, attributed to the new compound $\text{Cp}^*\text{Ti}\{\text{PhC}(\text{N}^i\text{Pr})_2\}\{\text{NC}(\text{NO}^t\text{Bu})\text{C}_6\text{FH}_3\text{N}(\text{Xyl})\text{C}\}(\text{F})$ (**22**), the analogue of **20**. However, the rate of the reaction was slow and after 5 days had only reached 70% completion. At this stage significant amounts of other (unknown) products had also formed and it was decided not to scale up this reaction. The slower rate of reaction of **21** in comparison to that of **19** is attributed to the decreased electrophilicity of the 2,6- $\text{C}_6\text{H}_3\text{F}_2$ ring in the former in comparison to that of C_6F_5 .

Reaction with $\text{B}(\text{Ar}^{\text{F}_5})_3$. Group 4 hydrazides $\text{M}(\text{N}_2^{\text{R}}\text{N}^{\text{Py}})(\text{NNPh}_2)(\text{py})$ readily form zwitterionic N_α adducts of the type $\text{M}(\text{N}_2^{\text{R}}\text{N}^{\text{Py}})\{\eta^2\text{-N}(\text{NPh}_2)\text{B}(\text{Ar}^{\text{F}_5})_3\}$ (**23**; $\text{M} = \text{Ti}, \text{Zr}, \text{Hf}, \text{R} = \text{SiMe}_3, \text{SiMe}_2^t\text{Bu}$) with $\text{B}(\text{Ar}^{\text{F}_5})_3$.^{2s,3c} In an extension of this chemistry we recently found that $\text{Cp}^*\text{Ti}\{\text{PhC}(\text{N}^i\text{Pr})_2\}(\text{NO}^t\text{Bu})$ (**1**) reacts with an excess of $\text{B}(\text{Ar}^{\text{F}_5})_3$, but in this case the reaction is accompanied by 2-methylpropene elimination from the *O-tert*-butyl group and formation of a HNO (nitroxyl) ligand with $\text{B}(\text{Ar}^{\text{F}_5})_3$ stabilization (**24**).^{7c} 2-Methylpropene elimination from cationic group 4 complexes containing either *tert*-butoxy ligands³⁹ or ligands with $-\text{O}^t\text{Bu}$ substituents such as Carpentier's cationic *tert*-butyl enolate systems is not uncommon.⁴⁰ We were therefore interested in examining the corresponding reaction of **5**.



Addition of $\text{B}(\text{Ar}^{\text{F}_5})_3$ to **5** in C_6D_6 at room temperature led to consumption of ca. 1 equiv. of borane after 7 h and formation of two new compounds, **25** (major, 86%) and **26** (minor, 14%), together with a small amount of 2-methylpropene (Scheme 7). In addition to the expected new signals in the ¹H and ¹⁹F NMR spectra for **25**, a new ¹¹B NMR resonance was observed at –7 ppm, indicative of four-coordinate boron⁴¹ and N coordination of $\text{B}(\text{Ar}^{\text{F}_5})_3$. Compound **25** is tentatively assigned as $\text{Cp}^*\text{Ti}\{\text{PhC}(\text{N}^i\text{Pr})_2\}\{\text{N}(\text{B}(\text{Ar}^{\text{F}_5})_3)\text{C}(\text{Ar}^{\text{F}_5})\text{N}(\text{O}^t\text{Bu})\}$, as shown in

Scheme 7. Reactions of

 $\text{Cp}^*\text{Ti}\{\text{PhC}(\text{N}^i\text{Pr})_2\}\{\text{NC}(\text{Ar}^{\text{F}_5})\text{NO}^t\text{Bu}\}$ (**5**) with $\text{B}(\text{Ar}^{\text{F}_5})_3$


Scheme 7 with a labile $\kappa^2\text{N,N}'$ -borataamidinate-type ligand, formed by addition of the borane to the N_α atom of **5** (cf. the corresponding N_α adducts **23** and **24**, which have similar ^{11}B NMR shifts). Further characterization and isolation of **25** was complicated by its instability toward elimination of 2-methylpropene and emergence of $\text{Cp}^*\text{Ti}\{\text{PhC}(\text{N}^i\text{Pr})_2\}\{\text{ON}(\text{B}\{\text{Ar}^{\text{F}_5}\}_3)\text{C}(\text{Ar}^{\text{F}_5})\text{N}(\text{H})\text{B}\{\text{Ar}^{\text{F}_5}\}_3\}$ (**26**). Formation of **26** was relatively slow at room temperature, but the compound could nonetheless be isolated in analytically pure form, albeit only in 26% yield, after heating a mixture of **5** and 2 equiv of the borane in C_6H_6 for 4 days at $70\text{ }^\circ\text{C}$. We were not able to obtain diffraction-quality crystals of **26**, and the structure is assigned by analogy to those of **23** and **24** on the basis of the spectroscopic and other analytical data.

The room-temperature ^1H NMR spectrum of **26** is consistent with a C_1 -symmetric complex. In addition to resonances for the isopropyl, Cp^* , and phenyl groups, a slightly broad singlet at δ 6.67 ppm (integral 1 H), which couples to the C_{ipso} of $(\text{H})\text{NCAr}^{\text{F}_5}\text{NO}$ and also to $(\text{H})\text{NCAr}^{\text{F}_5}\text{N}$, was assigned to NH (the corresponding $\nu(\text{N}-\text{H})$ is found at 3393 cm^{-1} in the IR spectrum). The room-temperature ^{19}F NMR spectrum was very broad at room temperature, but when the temperature was lowered to $-60\text{ }^\circ\text{C}$ the appearance of at least 22 multiplets (some overlapping) qualitatively confirmed the presence of 2 equiv of $\text{B}(\text{Ar}^{\text{F}_5})_3$ in **26**. The room-temperature ^{11}B NMR spectrum showed a single resonance δ -7 ppm, which broadened into the baseline on cooling to $-80\text{ }^\circ\text{C}$. Taken together, the ^{19}F and ^{11}B NMR variable-temperature spectra suggest that at room temperature the two $\text{B}(\text{Ar}^{\text{F}_5})_3$ groups are in dynamic exchange on the NMR time scale, but unfortunately low-temperature limiting spectra could not be obtained. The loss of 2-methylpropene from **25** to form **26** is reminiscent of the reactions of **1** to form **24**.

CONCLUSIONS

The first reactivity study of the benzimidamido ligand in $\text{Cp}^*\text{Ti}\{\text{PhC}(\text{N}^i\text{Pr})_2\}\{\text{NC}(\text{Ar}^{\text{F}_5})\text{NO}^t\text{Bu}\}$ (**5**) has allowed access to a range of stable $[2 + 2]$ cycloaddition intermediates which were isolated in good yields with CO_2 (forming **7**), isocyanates (forming **10**), and a series of aryl aldehydes (forming **13a–f**). The reactions with aryl aldehydes were reversible and allowed quantitative assessment of the relative stability of the

corresponding metallacycles as a function of the ring substituents. Upon heating, **10** and **13a–f** gave $^t\text{BuNCNC}(\text{Ar}^{\text{F}_5})\text{NO}^t\text{Bu}$ (**8**) and $(4\text{-C}_6\text{H}_4\text{X})\text{C}\{\text{NC}(\text{Ar}^{\text{F}_5})\text{NO}^t\text{Bu}\}\text{H}$ (**14a–f**), respectively, via a stereospecific extrusion reaction. Reaction of **5** with $\text{HC}(\text{O})\text{NMe}_2$ was more facile, yielding $\text{Me}_2\text{NC}\{\text{NC}(\text{Ar}^{\text{F}_5})\text{NO}^t\text{Bu}\}\text{H}$ (**16**) within 1 h at room temperature. DFT calculations on **14a–f** and **16** probed the electronic structures of these compounds and the relative energies of their conformers. The reaction of **5** with $^t\text{BuNC}$ and XylNC gave σ adducts, $\text{Cp}^*\text{Ti}\{\text{PhC}(\text{N}^i\text{Pr})_2\}\{\text{NC}(\text{Ar}^{\text{F}_5})\text{NO}^t\text{Bu}\}(\text{CNR})$ ($\text{R} = ^t\text{Bu}$ (**18**), Xyl (**19**)), and the latter underwent further reaction, yielding $\text{Cp}^*\text{Ti}\{\text{PhC}(\text{N}^i\text{Pr})_2\}\{\text{NC}(\text{NO}^t\text{Bu})\text{C}_6\text{F}_4\text{N}(\text{Xyl})\text{C}\}(\text{F})$ (**20**) following a C–F activation mechanism. Reaction of **5** with 2 equiv of $\text{B}(\text{Ar}^{\text{F}_5})_3$ resulted in $\text{Cp}^*\text{Ti}\{\text{PhC}(\text{N}^i\text{Pr})_2\}\{\text{ON}(\text{B}\{\text{Ar}^{\text{F}_5}\}_3)\text{C}(\text{Ar}^{\text{F}_5})\text{N}(\text{H})\text{B}\{\text{Ar}^{\text{F}_5}\}_3\}$ (**26**) following loss of 2-methylpropene. In all of these reactions, the new organometallic or organic products contain the benzimidamide moiety, $\text{NC}(\text{Ar}^{\text{F}_5})\text{NO}^t\text{Bu}$, derived initially from the *tert*-butoxyimido ligand of $\text{Cp}^*\text{Ti}\{\text{PhC}(\text{N}^i\text{Pr})_2\}(\text{NO}^t\text{Bu})$ (**1**) and $\text{Ar}^{\text{F}_5}\text{CN}$, and thus these represent new multicomponent coupling reactions.

EXPERIMENTAL SECTION

General Methods and Instrumentation. All manipulations were carried out using standard Schlenk line or drybox techniques under an atmosphere of argon or dinitrogen. Solvents were either degassed by sparging with dinitrogen and dried by passing through a column of the appropriate drying agent or refluxed over sodium (toluene), potassium (THF), or Na/K alloy (Et_2O) and distilled. Deuterated solvents were dried over sodium (C_6D_6 and toluene- d_8), distilled under reduced pressure, and stored under argon in Teflon valve ampoules. Unless stated, NMR samples were prepared under dinitrogen in 5 mm Wilmad 507-PP tubes fitted with J. Young Teflon valves. ^1H , $^{13}\text{C}\{^1\text{H}\}$, $^{13}\text{C}\{^{19}\text{F}\}$, ^{11}B , and ^{19}F spectra were recorded on Varian Mercury-VX 300 or Bruker Avance III 500 spectrometers or on a Bruker AVX 500 spectrometer fitted with a ^{13}C cryoprobe. ^1H , $^{13}\text{C}\{^1\text{H}\}$, and $^{13}\text{C}\{^{19}\text{F}\}$ spectra are referenced internally to residual protio solvent (^1H) or solvent (^{13}C) resonances and are reported relative to tetramethylsilane (δ 0 ppm). ^{19}F and ^{11}B spectra were referenced externally to CFCl_3 and $\text{Et}_2\text{O}\cdot\text{BF}_3$, respectively. Assignments were confirmed as necessary with the use of two-dimensional $^1\text{H}-^1\text{H}$, $^{13}\text{C}-^1\text{H}$, and $^{13}\text{C}-^{19}\text{F}$ NMR correlation experiments. IR spectra were recorded on a Perkin-Elmer Paragon 1000 FTIR or a Thermo Scientific Nicolet iS5 FTIR spectrometer and samples prepared in a drybox using NaCl plates as a Nujol mull or as a thin film. UV–visible spectra were recorded on a T60U spectrometer at 298 K in 1 cm path length cuvettes with $[\text{14 or 16}] = 5.17\text{ }\mu\text{mol dm}^{-3}$ in either *n*-hexane or MeOH. Mass spectra were recorded by the mass spectrometry service of Oxford University's Department of Chemistry. Elemental analyses were carried out by the Elemental Analysis Service at the London Metropolitan University.

Starting Materials. $\text{Cp}^*\text{Ti}\{\text{PhC}(\text{N}^i\text{Pr})_2\}(\text{NO}^t\text{Bu})$ (**1**) and $\text{Cp}^*\text{Ti}\{\text{PhC}(\text{N}^i\text{Pr})_2\}\{\text{NC}(\text{Ar}^{\text{F}_5})\text{NO}^t\text{Bu}\}$ (**5**) were synthesized according to published procedures.^{7c} $\text{B}(\text{Ar}^{\text{F}_5})_3$ was provided by LANXESS Elastomers BV. All other reagents were purchased from commercial suppliers and (for liquid reagents) degassed before use, unless specified otherwise. $\text{Ar}^{\text{F}_5}\text{CN}$ and $\text{Ar}'\text{NCO}$ ($\text{Ar}' = 2,6\text{-C}_6\text{H}_3\text{Pr}_2$) were dried over CaH_2 and distilled before use. $\text{HC}(\text{O})\text{NMe}_2$ was degassed by sparging with dinitrogen and dried by passing through a column of activated alumina.

In Situ Synthesis of $\text{Cp}^*\text{Ti}\{\text{PhC}(\text{N}^i\text{Pr})_2\}\{\text{NC}(\text{Ar}^{\text{F}_5})\text{NO}^t\text{Bu}\}$ (5**).** In all reactions $\text{Cp}^*\text{Ti}\{\text{PhC}(\text{N}^i\text{Pr})_2\}\{\text{NC}(\text{Ar}^{\text{F}_5})\text{NO}^t\text{Bu}\}$ (**5**) was synthesized in situ for convenience. An example of the method is as follows. To a stirred solution of $\text{Cp}^*\text{Ti}\{\text{PhC}(\text{N}^i\text{Pr})_2\}(\text{NO}^t\text{Bu})$ (**1**; 0.350 g, 0.739 mmol) in benzene (5 mL) was added $\text{Ar}^{\text{F}_5}\text{CN}$ (93.2 μL , 0.739 mmol), all at room temperature. An immediate color change from dark green to lime green was observed, and the solution was stirred for 15 min, quantitatively forming **5**.

Cp*Ti{PhC(NⁱPr)₂}₂{OC(O)N(C{Ar^{F5}})NOⁱBu} (7). A solution of Cp*Ti{PhC(NⁱPr)₂}₂{NC(Ar^{F5})NOⁱBu} (5; 0.422 g, 0.634 mmol) in benzene (5 mL) was freeze–pump–thawed three times. The solution was then exposed to CO₂ at a pressure of ca. 1.5 atm at room temperature. After 1 h the volatiles were removed under reduced pressure to afford 7 as a dark green solid which was washed with cold pentane (3 × 5 mL, –78 °C), filtered, and dried in vacuo. Yield: 0.296 g (66%). ¹H NMR (C₆D₆, 499.9 MHz, 293 K): δ 7.23 (1 H, d, ³J = 7.5 Hz, *o*-C₆H₅), 7.05–6.92 (4 H, m, *o*_b-C₆H₅, *m*-C₆H₅, and *p*-C₆H₅), 4.20 (1 H, app sept, app ³J = 6.5 Hz, NCH₃MeMe), 3.20 (1 H, app sept, app ³J = 6.5 Hz, NCH₃MeMe), 2.16 (15 H, s, C₅Me₅), 1.28 (9 H, s, NOCMe₃), 1.07 (3 H, d, ³J = 6.5 Hz, NCH₃MeMe), 1.02 (3 H, d, ³J = 6.5 Hz, NCH₃MeMe), 1.00 (3 H, d, ³J = 7.0 Hz, NCH₃MeMe), 0.89 (3 H, d, ³J = 6.5 Hz, NCH₃MeMe) ppm. ¹³C{¹H} NMR (C₆D₆, 125.7 MHz, 293 K): δ 171.6 (PhCN₂), 155.8 (OC(O)N), 146.2 (NC(C₆F₅)N), 144.0 (1 C, d, ¹J_{C–F} = 246.2 Hz, *o*-C₆F₅), 143.5 (1 C, d, ¹J_{C–F} = 242.8 Hz, *o*_b-C₆F₅), 141.2 (1 C, d, ¹J_{C–F} = 251.4 Hz, *p*-C₆F₅), 138.0 (1 C, d, ¹J_{C–F} = 248.8 Hz, *m*_a-C₆F₅), 137.8 (1 C, d, ¹J_{C–F} = 248.9 Hz, *m*_b-C₆F₅), 133.0 (*i*-C₆H₅), 132.2 (C₅Me₅), 129.5 (*p*-C₆H₅), 128.6 (*o*_b-C₆H₅), 128.5 (*o*_a-C₆H₅), 128.1 (overlapping with solvent *m*-C₆H₅), 112.3 (1 C, appt of t, ²J_{C–F} = 19.8 Hz, ³J_{C–F} = 3.8 Hz, *i*-C₆F₅), 78.0 (NOCMe₃), 51.4 (NCH₃MeMe), 50.5 (NCH₃MeMe), 27.8 (NOCMe₃), 25.3 (NCH₃MeMe), 25.1 (NCH₃MeMe), 24.8 (NCH₃MeMe), 24.0 (NCH₃MeMe), 13.0 (C₅Me₅) ppm. ¹⁹F{¹H} NMR (C₆D₆, 282.1 MHz, 293 K): δ –137.7 (1 F, app d, app ³J = 23.1 Hz, *o*_a-C₆F₅), –143.3 (1 F, app d, app ³J = 23.1 Hz, *o*_b-C₆F₅), –156.2 (1 F, t, ³J = 21.4 Hz, *p*-C₆F₅), –164.6 (1 F, m, *m*_a-C₆F₅), –164.9 (1 F, m, *m*_b-C₆F₅) ppm. IR (NaCl plates, Nujol mull, cm^{–1}): 1690 (s), 1655 (w), 1578 (w), 1521 (m), 1496 (s), 1424 (m), 1362 (s), 1337 (m), 1293 (w), 1259 (w), 1218 (m), 1176 (m), 1143 (w), 1110 (m), 1070 (w), 1044 (w), 1023 (m), 990 (m), 954 (m), 921 (m), 901 (w), 786 (w), 707 (w). Anal. Found (calcd for C₃₅H₄₃F₅N₄O₃Ti): C, 58.89 (59.16); H, 6.29 (6.10); N, 7.76 (7.88).

NMR Tube Scale Synthesis of Cp*Ti{PhC(NⁱPr)₂}₂{OC(O)N(C{Ar^{F5}})NOⁱBu} (8). A solution of Cp*Ti{PhC(NⁱPr)₂}₂{OC(O)N(C{Ar^{F5}})NOⁱBu} (7; 25.0 mg, 0.0351 mmol) in C₆D₆ (0.35 mL) in a 0.77 mm New Era NE-HP5-M NMR tube equipped with a controlled-atmosphere valve was freeze–pump–thawed three times. The solution was then exposed to CO₂ at a pressure of ca. 1.5 atm at room temperature. The reaction was monitored by ¹H and ¹⁹F NMR spectroscopy. The ¹H NMR spectrum recorded after 5 days at room temperature indicated that the reaction had reached 63% conversion to 8. 8 was characterized by ¹H, ¹³C, and ¹⁹F NMR spectroscopy. ¹H NMR (C₆D₆, 499.9 MHz, 293 K): δ 7.03–6.92 (3 H, m, *m*-C₆H₅ and *p*-C₆H₅), 6.82 (1 H, m, *o*_a-C₆H₅), 6.65 (1 H, d, ³J = 7.0 Hz, *o*_b-C₆H₅), 3.41 (2 H, app sept, app ³J = 6.5 Hz, NCHMeMe), 1.99 (15 H, s, C₅Me₅), 1.37 (9 H, s, NOCMe₃), 0.95 (6 H, d, ³J = 6.5 Hz, NCHMeMe), 0.93 (6 H, d, ³J = 6.5 Hz, NCHMeMe) ppm. ¹³C{¹H} NMR (C₆D₆, 125.7 MHz, 293 K): δ 171.7 (PhCN₂), 152.8 (OC(O)N), 145.0 (2 C, d, ¹J_{C–F} = 249.5 Hz, *o*-C₆F₅), 141.9 (1 C, d, ¹J_{C–F} = 254.6 Hz, *p*-C₆F₅), 137.9 (2 C, d, ¹J_{C–F} = 250.8 Hz, *m*-C₆F₅), 137.3 (NC(C₆F₅)N), 132.4 (C₅Me₅), 132.3 (*i*-C₆H₅), 129.4 (*p*-C₆H₅), 128.1 (overlapping with solvent *o*_b-C₆H₅, *m*-C₆H₅), 127.7 (*o*_a-C₆H₅), 109.2 (1 C, app t of t, ²J_{C–F} = 17.6 Hz, ³J_{C–F} = 3.3 Hz, *i*-C₆F₅), 81.5 (NOCMe₃), 51.6 (NCHMeMe), 27.7 (NOCMe₃), 24.7, 24.6 (NCHMeMe), 12.8 (C₅Me₅) ppm. ¹⁹F{¹H} NMR (C₆D₆, 282.1 MHz, 293 K): δ –134.1 (2 F, app d, app ³J = 18.9 Hz, *o*-C₆F₅), –154.2 (1 F, app t of t, app ³J = 21.4 Hz, ⁴J = 3.1 Hz, *p*-C₆F₅), –164.1 (2 F, m, *m*-C₆F₅) ppm.

NMR Tube Scale Reaction of Cp*Ti{PhC(NⁱPr)₂}₂{NC(Ar^{F5})NOⁱBu} (5) with CS₂. To a solution of Cp*Ti{PhC(NⁱPr)₂}₂{NC(Ar^{F5})NOⁱBu} (5; 14.4 mg, 0.0215 mmol) in C₆D₆ (0.5 mL) in an NMR tube equipped with a J. Young Teflon valve was added CS₂ (1.55 μL, 0.0258 mmol) at room temperature. The reaction was monitored by ¹H and ¹⁹F NMR spectroscopy. After 15 days Cp*Ti{PhC(NⁱPr)₂}₂{N(OⁱBu)C(S)S} (9) and Ar^{F5}CN were observed in 70% yield. Resonances attributed to 9 were consistent with values reported in the literature.^{7c}

Cp*Ti{PhC(NⁱPr)₂}₂{NC(Ar^{F5})NOⁱBu}C(NⁱBu)O} (10). To a solution of Cp*Ti{PhC(NⁱPr)₂}₂{NC(Ar^{F5})NOⁱBu} (5; 0.352 g, 0.528

mmol) in diethyl ether (5 mL) was added ^tBuNCO (60.3 μL, 0.528 mmol), all at room temperature. A gradual color change from lime green to dark yellow was observed, and the solution was stirred for 6.5 h. Volatiles were then removed under reduced pressure to afford 11 as a brown powder which was dried in vacuo. Yield: 0.261 g (65%). ¹H NMR (C₆D₆, 499.9 MHz, 293 K): δ 7.37 (1 H, d, ³J = 7.5 Hz, *o*_a-C₆H₅), 7.00 (4 H, m, overlapping *o*_b-C₆H₅, *m*-C₆H₅, and *p*-C₆H₅), 4.20 (1 H, app sept, app ³J = 7.0 Hz, NCH₃MeMe), 3.24 (1 H, app sept, app ³J = 6.5 Hz, NCH₃MeMe), 2.17 (15 H, s, C₅Me₅), 1.33 (9 H, s, NOCMe₃), 1.33 (9 H, s, NOCMe₃), 1.15 (3 H, d, ³J = 7.0 Hz, NCH₃MeMe), 0.97 (9 H, m, overlapping NCH₃MeMe, NCH₃MeMe, NCH₃MeMe) ppm. ¹³C{¹H} NMR (C₆D₆, 125.7 MHz, 293 K): δ 170.6 (PhCN₂), 148.2, 146.7 (OCN and NC(Ar^{F5})N), 133.9 (*i*-C₆H₅), 130.3 (C₅Me₅), 129.3 (*m*-C₆H₅), 128.7 (*o*_a-C₆H₅), 128.7 (*o*_b-C₆H₅), 128.6 (*p*-C₆H₅), 113.9 (1 C, app t, app ²J_{C–F} = 21.3 Hz, *i*-C₆F₅), 77.8 (NOCMe₃), 51.0 (NOCMe₃), 50.8 (NCH₃MeMe), 50.1 (NCH₃MeMe), 32.2 (NOCMe₃), 27.8 (NOCMe₃), 25.5 (NCH₃MeMe), 25.6, 24.6, 24.5 (NCH₃MeMe, NCH₃MeMe, NCH₃MeMe), 12.9 (C₅Me₅) ppm. ¹³C NMR (HMQC ¹⁹F-observed, C₆D₆, 282.1 MHz, 293 K): δ 144.2 (*o*_a-C₆F₅), 142.8 (*o*_b-C₆F₅), 140.6 (*p*-C₆F₅), 137.6 (*m*-C₆F₅), 137.3 (*m*-C₆F₅) ppm. ¹⁹F{¹H} NMR (C₆D₆, 282.1 MHz, 293 K): δ –135.3 (1 H, m, *o*_a-C₆F₅), –143.6 (1 H, m, *o*_b-C₆F₅), –159.7 (1 H, m, *p*-C₆F₅), –166.9 (1 H, m, *m*_a-C₆F₅), –167.2 (1 H, m, *m*_b-C₆F₅) ppm. IR (NaCl plates, Nujol mull, cm^{–1}): 1631 (s), 1579 (m), 1516 (s), 1494 (s), 1483 (m), 1453 (s), 1423 (m), 1401 (m), 1360 (s), 1335 (m), 1289 (w), 1261 (m), 1221 (m), 1196 (w), 1174 (m), 1148 (w), 1101 (m), 1062 (m), 1020 (m), 990 (m), 967 (m), 943 (w), 899 (w), 861 (w), 797 (br w), 732 (w), 704 (w). EI-MS: *m/z* 666 [Cp*Ti{PhC(NⁱPr)₂}₂{NC(Ar^{F5})NOⁱBu}]⁺ (5%); Anal. Found (calcd for C₃₉H₅₂F₅N₅O₃Ti): C, 60.99 (61.17); H, 6.72 (6.84); N, 8.98 (9.15).

^tBuNCNC(Ar^{F5})NOⁱBu (12). To a solution of Cp*Ti{PhC(NⁱPr)₂}₂{NC(Ar^{F5})NOⁱBu} (5; 0.493 g, 0.739 mmol) in benzene (5 mL) was added ^tBuNCO (84.4 μL, 0.739 mmol), all at room temperature. A gradual color change from lime green to dark yellow was observed, and the solution was stirred for 3 h before being heated to 65 °C and stirred for a further 16 h. A further color change to yellow was observed. Volatiles were then removed under reduced pressure to afford [Cp*Ti{PhC(NⁱPr)₂}₂(μ-O)]₂ (11) and 12 as a brown oily solid. The resultant solid was extracted into diethyl ether (3 × 5 mL, –78 °C), and the volatiles were removed under reduced pressure. The resultant brown oil was then distilled (100 °C, 8 × 10^{–2} mbar, 4.5 h) onto a dry ice/acetone cold finger, affording 12 as a yellow oil. Yield: 0.190 g (71%). ¹H NMR (C₆D₆, 499.9 MHz, 293 K): δ 1.25 (9 H, s, NOCMe₃), 1.00 (9 H, s, NOCMe₃) ppm. ¹³C{¹H} NMR (C₆D₆, 125.7 MHz, 293 K): δ 143.6 (2 C, d, ¹J_{C–F} = 249.3 Hz, *o*-C₆F₅), 141.9 (1 C, d, ¹J_{C–F} = 253.8 Hz, *p*-C₆F₅), 139.8 (NCN or NC(Ar^{F5})N), 137.8 (2 C, d, ¹J_{C–F} = 251.1 Hz, *m*-C₆F₅), 133.0 (NC(Ar^{F5})N or NCN), 108.6 (1 C, t of d, ²J_{C–F} = 20.1 Hz, ³J_{C–F} = 3.9 Hz, *i*-C₆F₅), 80.6 (NOCMe₃), 58.3 (NOCMe₃), 31.0 (NOCMe₃), 27.4 (NOCMe₃) ppm. ¹⁹F{¹H} NMR (C₆D₆, 282.1 MHz, 293 K): δ –138.2 (2 H, app d, app ³J = 13.0 Hz, *o*-C₆F₅), –152.7 (1 H, t, ³J = 21.7 Hz, *p*-C₆F₅), –161.9 (2 H, m, *m*-C₆F₅) ppm. IR (NaCl plates, thin film, cm^{–1}): 2977 (m), 2933 (w), 2872 (w), 2141 (s), 1653 (m), 1594 (br, m), 1521 (s), 1499 (s), 1457 (m), 1437 (m), 1389 (w), 1366 (m), 1317 (m), 1261 (w), 1238 (m), 1204 (s), 1173 (m), 1116 (w), 1103 (w), 1088 (m), 1071 (w), 1034 (w), 991 (s), 905 (m), 880 (m), 837 (w), 795 (w), 745 (w), 727 (w), 692 (w), 668 (w), 636 (w), 586 (w), 567 (w). FI-HRMS found (calcd for [C₁₆H₁₈F₅N₃O]⁺): 363.1380 (363.1370).

Cp*Ti{PhC(NⁱPr)₂}₂{NC(Ar^{F5})NOⁱBu}C(Ph)(H)O} (13a). To a solution of Cp*Ti{PhC(NⁱPr)₂}₂{NC(Ar^{F5})NOⁱBu} (5; 0.422 g, 0.634 mmol) in diethyl ether (5 mL) was added PhC(O)H (64.4 μL, 0.634 mmol), all at room temperature. An immediate color change from lime green to brown was observed, and the solution was stirred for 15 min. Volatiles were then removed under reduced pressure to afford 13a as a brown powder which was dried in vacuo. Yield: 0.403 g (82%). Diffraction-quality crystals were grown from a saturated hexane solution at 4 °C. ¹H NMR (C₆D₆, 299.9 MHz, 293 K): δ 7.47 (1 H, d, ³J = 7.2 Hz, *o*_a-C₆H₅CN₂), 7.22 (1 H, d, ³J = 6.9 Hz, *o*_b-C₆H₅CN₂), 7.11 (3 H, m, overlapping *m*-C₆H₅CN₂ and *p*-C₆H₅), 6.93 (5 H, m, overlapping *p*-C₆H₅CN₂, *o*-C₆H₅, and *m*-C₆H₅), 5.99 (1 H, d, J_{H–F} =

2.1 Hz, PhC(H)), 4.50 (1 H, app sept, app $^3J = 6.6$ Hz, NCH₃MeMe), 3.44 (1 H, app sept, app $^3J = 6.6$ Hz, NCH₃MeMe), 2.28 (15 H, s, C₃Me₃), 1.32 (3 H, d, $^3J = 6.6$ Hz, NCH₃MeMe), 1.27 (9 H, s, OCM₃), 1.19 (3 H, d, $^3J = 6.9$ Hz, NCH₃MeMe), 0.90 (3 H, d, $^3J = 6.9$ Hz, NCH₃MeMe), 0.83 (3 H, d, $^3J = 6.6$ Hz, NCH₃MeMe) ppm. ¹³C{¹H} NMR (C₆D₆, 75.4 MHz, 293 K): δ 167.9 (PhCN₂), 148.7 (NC(Ar^{F5})NO^tBu), 145.6 (*i*-C₆H₅), 135.6 (*i*-C₆H₅CN₂), 129.7 (*o*-C₆H₅CN₂), 128.9 (*p*-C₆H₅), 128.5 (*o*_o-C₆H₅CN₂), 127.9 (*m*-C₆H₅CN₂), 127.8 (*m*-C₆H₅), 127.7 (overlapping with solvent *p*-C₆H₅CN₂), 127.5 (C₃Me₃), 126.9 (*o*-C₆H₅), 112.6 (1 C, *m*, *i*-C₆F₅), 83.4 (1 C, d, $J_{C-F} = 1.2$ Hz, PhC(H)), 76.9 (OCMe₃), 49.9 (NCH₃MeMe), 48.9 (NCH₃MeMe), 28.2 (OCMe₃), 25.7 (NCH₃MeMe), 25.4 (NCH₃MeMe), 24.8 (NCH₃MeMe), 24.6 (NCH₃MeMe), 12.4 (C₃Me₃) ppm. ¹³C NMR (HMOC ¹⁹F-observed, C₆D₆, 282.1 MHz, 293 K): δ 142.5 (*o*_a-C₆F₅), 141.9 (*o*_b-C₆F₅), 140.7 (*p*-C₆F₅), 137.3 (*m*_a-C₆F₅), 137.2 (*m*_b-C₆F₅) ppm. ¹⁹F{¹H} NMR (C₆D₆, 282.1 MHz, 293 K): δ -134.8 (1 F, *m*, *o*_a-C₆F₅), -141.7 (1 F, *m*, *o*_b-C₆F₅), -156.6 (1 F, *m*, *p*-C₆F₅), -164.1 (1 F, *m*, *m*_a-C₆F₅), -164.8 (1 F, *m*, *m*_b-C₆F₅) ppm. IR (NaCl plates, Nujol mull, cm⁻¹): 1653 (w), 1550 (m), 1519 (m), 1495 (s), 1363 (m), 1358 (m), 1346 (m), 1289 (w), 1267 (w), 1260 (w), 1230 (w), 1221 (w), 1196 (m), 1169 (w), 1151 (w), 1133 (w), 1112 (m), 1085 (w), 1059 (m), 1021 (m), 994 (m), 987 (m), 959 (m), 922 (w), 905 (w), 893 (w), 795 (w), 781 (w), 730 (w), 721 (w), 711 (w), 704 (m), 696 (w), 642 (m), 615 (w), 590 (w), 576 (w), 537 (w). Anal. Found (calcd for C₄₁H₄₉F₅N₄O₂Ti): C, 63.60 (63.73); H, 6.28 (6.39); N, 7.18 (7.25).

Equilibrium Constants. A total of 0.5 mL of C₆D₆ was used in each experiment. The general procedure is as follows. To a solution of Cp*Ti{PhC(NⁱPr)₂}₂{N(C{Ar^{F5}}NO^tBu)C(Ph)(H)O} (13a; 10.0 mg, 0.0129 mmol) in C₆D₆ in an NMR tube equipped with a J. Young Teflon valve was added ArC(O)H (0.0129 mmol), in C₆D₆ where necessary, all at room temperature. The reaction was monitored by ¹H (relaxation delay 100 s) and ¹⁹F NMR spectroscopy. The ratios of reagents and products were calculated by measuring the integrals of the free and bound ArCH hydrogens, giving the required equilibrium constants (in the case of 4-C₆H₄Me and 4-C₆H₄OMe it was necessary to integrate the methyl groups of the isopropyl substituents instead).

Kinetic Measurements. The general procedure is as follows. Cp*Ti{PhC(NⁱPr)₂}₂{N(C{Ar^{F5}}NO^tBu)C(Ar)(H)O} (13a-f; 0.0129 mmol) was dissolved in C₆D₆ (0.6 mL) and transferred to a NMR tube equipped with a J. Young Teflon valve. The NMR probe was warmed to 70 °C and the sample added before being locked and shimmed. After the sample was allowed to thermally equilibrate (ca. 10 min), the shimming was checked and an array set up recording a spectrum of four scans every 120 s. The ratios of the species were calculated by measuring the integrals of the ArCH protons. First-order rate constants were obtained from linear plots of ln([13a-f]_t/[13a-f]₀) vs time.

NMR Tube Scale Reaction of Cp*Ti{PhC(NⁱPr)₂}₂{NC(Ar^{F5})NO^tBu} (5) with PhC(O)H and (4-C₆H₄NMe₂)C(O)H (1:1 Ratio). To a solution of Cp*Ti{PhC(NⁱPr)₂}₂{NC(Ar^{F5})NO^tBu} (5; 21.1 mg, 0.0317 mmol) in C₆D₆ (0.3 mL) in an NMR tube equipped with a J. Young Teflon valve was added a premixed solution of PhC(O)H (3.22 μL, 0.0317 mmol) and (4-C₆H₄NMe₂)C(O)H (4.73 mg, 0.0317 mmol) in C₆D₆ (0.3 mL) at room temperature. A color change from lime green to brown was observed. After 1 h 45 min at room temperature, the solution was heated to 65 °C. After 20.5 h PhC{NC(Ar^{F5})NO^tBu}H (14a) and (4-C₆H₄NMe₂)C{NC(Ar^{F5})NO^tBu}H (14e) were observed, alongside [Cp*Ti{PhC(NⁱPr)₂}₂(μ-O)]₂ (11), in the ¹H NMR spectrum in a 64:36 ratio, respectively.

PhC{NC(Ar^{F5})NO^tBu}H (14a). To a solution of Cp*Ti{PhC(NⁱPr)₂}₂{NC(Ar^{F5})NO^tBu} (5; 0.301 g, 0.452 mmol) in benzene (5 mL) was added PhC(O)H (45.9 μL, 0.452 mmol), all at room temperature. An immediate color change from lime green to brown was observed, and the solution was stirred for 15 min before being heated to 70 °C and stirred for a further 19 h. A further color change to yellow was observed. Volatiles were then removed under reduced pressure to afford [Cp*Ti{PhC(NⁱPr)₂}₂(μ-O)]₂ (11) and 14a as a yellow-brown oily solid. The resultant solid was sublimed (80 °C, 8 × 10⁻² mbar, 2 h) onto a dry ice/acetone cold finger, affording 14a as a

white solid. Yield: 0.104 g (62%). ¹H NMR (C₆D₆, 499.9 MHz, 293 K): δ 8.50 (1 H, s, PhC(NⁱPr)H), 7.69 (2 H, m, *o*-C₆H₅), 7.05–6.97 (3 H, m, overlapping *m*-C₆H₅ and *p*-C₆H₅), 1.30 (9 H, s, NOCMe₃). ¹³C{¹H} NMR (C₆D₆, 125.7 MHz, 293 K): δ 162.0 (PhC(NⁱPr)H), 149.2 (NC(Ar^{F5})NO^tBu), 143.9 (2 C, d, $J_{C-F} = 251.3$ Hz, *o*-C₆F₅), 141.9 (1 C, d overlapping with *o*-C₆F₅, $J_{C-F} = 253.8$ Hz, *p*-C₆F₅), 138.0 (2 C, d, $J_{C-F} = 252.5$ Hz, *m*-C₆F₅), 135.6 (*i*-C₆H₅), 132.5 (*p*-C₆H₅), 129.9 (*o*-C₆H₅), 129.0 (*m*-C₆H₅), 108.0 (1 C, t of d, $^2J_{C-F} = 20.0$ Hz, $^3J_{C-F} = 3.8$ Hz, *i*-C₆F₅), 81.2 (NOCMe₃), 27.5 (NOCMe₃) ppm. ¹⁹F{¹H} NMR (C₆D₆, 282.1 MHz, 293 K): δ -138.2 (2 F, *m*, *o*-C₆F₅), -152.7 (1 F, t of t, $^3J = 21.2$ Hz, $^4J = 2.3$ Hz, *p*-C₆F₅), -161.8 (2 F, *m*, *m*-C₆F₅) ppm. IR (NaCl plates, Nujol mull, cm⁻¹): 1657 (m), 1623 (m), 1602 (w), 1592 (w), 1579 (m), 1520 (s), 1497 (s), 1454 (m), 1434 (m), 1364 (m), 1323 (w), 1313 (w), 1296 (w), 1261 (w), 1243 (w), 1205 (m), 1187 (m), 1101 (m), 1073 (w), 998 (m), 985 (s), 970 (s), 905 (m), 892 (w), 858 (m), 798 (w), 766 (m), 707 (m), 695 (m), 668 (w), 615 (w), 597 (m), 582 (m). ESI⁺-HRMS found (calcd for [C₁₈H₁₅F₅N₂NaO, M + Na⁺]⁺): 393.0989 (393.0997). UV-vis: λ_{max}(*n*-hexane) 271 nm (ε = 3.0 × 10⁴ mol⁻¹ dm³ cm⁻¹); λ_{max}(MeOH) 284 nm (ε = 2.4 × 10⁴ mol⁻¹ dm³ cm⁻¹).

NMR Tube Scale Synthesis of Cp*Ti{PhC(NⁱPr)₂}₂{NC(Ar^{F5})NO^tBu}{OC(NMe₂)H} (15). To a solution of Cp*Ti{PhC(NⁱPr)₂}₂{N(C{Ar^{F5}}NO^tBu)} (5; 17.0 mg, 0.0256 mmol) in C₆D₆ (0.3 mL) in an NMR tube equipped with a J. Young Teflon valve was added Me₂NC(O)H (1.87 mg, 0.0256 mmol) in C₆D₆ (0.3 mL) at room temperature. A color change from lime green to red-brown was observed. The reaction was monitored by ¹H and ¹⁹F NMR spectroscopy. Within 5 min 15 was observed alongside Me₂NC{NC(Ar^{F5})NO^tBu}H (16) and [Cp*Ti{PhC(NⁱPr)₂}₂(μ-O)]₂ (11) in a 92:8 ratio. 15 was characterized by ¹H and ¹⁹F NMR spectroscopy. ¹H NMR (C₆D₆, 299.9 MHz, 293 K): δ 7.92 (1 H, br s, Me₂NC(H)), 7.32 (1 H, d, $^3J = 8.1$ Hz, *o*_a-C₆H₅), 7.21–6.98 (4 H, m, *o*_b-C₆H₅, *m*-C₆H₅, and *p*-C₆H₅), 3.40 (2 H, sept, $^3J = 6.6$ Hz, NCHMeMe), 2.36 (3 H, s, NMeMe), 2.22 (15 H, s, C₃Me₃), 1.95 (3 H, s, NMeMe), 1.40 (9 H, s, NOCMe₃), 0.86 (6 H, d, $^3J = 6.6$ Hz, NCHMeMe), 0.81 (6 H, d, $^3J = 6.6$ Hz, NCHMeMe) ppm. ¹⁹F{¹H} NMR (C₆D₆, 282.1 MHz, 293 K): δ -140.0 (2 F, *m*, *o*-C₆F₅), -158.2 (1 F, t, $^3J = 21.2$ Hz, *p*-C₆F₅), -164.0 (2 F, *m*, *m*-C₆F₅) ppm.

Me₂NC{NC(Ar^{F5})NO^tBu}H (16). To a solution of Cp*Ti{PhC(NⁱPr)₂}₂{NC(Ar^{F5})NO^tBu} (5; 0.351 g, 0.528 mmol) in benzene (5 mL) was added HC(O)NMe₂ (40.9 μL, 0.528 mmol), all at room temperature. An immediate color change from lime green to red-brown and then to yellow was observed, and the solution was stirred for 3 h. The solution was then filtered, and the volatiles were removed under reduced pressure to afford [Cp*Ti{PhC(NⁱPr)₂}₂(μ-O)]₂ (11) and 16 as a yellow-brown oily solid. The resultant solid was sublimed (80 °C, 8 × 10⁻² mbar, 3 h) onto a dry ice/acetone cold finger, affording 16 as a white solid. Yield: 0.114 g (64%). Diffraction-quality crystals were grown from the slow evaporation of a pentane solution at room temperature. ¹H NMR (C₆D₆, 499.9 MHz, 293 K): δ 7.79 (1 H, s, HC(N)NMe₂), 2.42 (3 H, s, HC(N)NMeMe), 1.90 (3 H, s, HC(N)NMeMe), 1.37 (9 H, s, NOCMe₃) ppm. ¹³C{¹H} NMR (C₆D₆, 125.7 MHz, 293 K): δ 152.8 (HC(N)NMe₂), 148.8 (NC(Ar^{F5})N), 143.9 (2 C, d, $J_{C-F} = 247.5$ Hz, *o*-C₆F₅), 141.2 (1 C, d, $J_{C-F} = 255.0$ Hz, *p*-C₆F₅), 137.9 (2 C, d, $J_{C-F} = 250.0$ Hz, *m*-C₆F₅), 112.1 (1 C, t of d, $^2J_{C-F} = 20.0$ Hz, $^3J_{C-F} = 3.8$ Hz, *i*-C₆F₅), 78.8 (NOCMe₃), 39.2 (HC(N)NMeMe), 33.9 (HC(N)NMeMe), 27.7 (NOCMe₃) ppm. ¹⁹F{¹H} NMR (C₆D₆, 282.1 MHz, 293 K): δ -140.2 (2 F, *m*, *o*-C₆F₅), -155.8 (1 F, t of t, $^3J = 21.2$ Hz, $^4J = 1.41$ Hz, *p*-C₆F₅), -163.3 (2 F, *m*, *m*-C₆F₅) ppm. IR (NaCl plates, Nujol mull, cm⁻¹): 1626 (s), 1565 (m), 1520 (m), 1497 (s), 1441 (m), 1419 (m), 1410 (w), 1397 (w), 1364 (s), 1317 (w), 1256 (w), 1232 (w), 1191 (m), 1113 (s), 1095 (m), 1064 (w), 1036 (w), 995 (s), 985 (m), 960 (m), 927 (w), 910 (m), 900 (w), 866 (w), 800 (w), 700 (m), 681 (w), 610 (w), 581 (w). ESI⁺-HRMS found (calcd for [C₁₄H₁₆F₅N₃NaO, M + Na⁺]⁺): 360.1102 (360.1106). UV-vis: dm³ cm⁻¹.

Cp*Ti{PhC(NⁱPr)₂}₂{NC(Ar^{F5})NO^tBu}(CNⁱBu) (18). To a solution of Cp*Ti{PhC(NⁱPr)₂}₂{NC(Ar^{F5})NO^tBu} (5; 0.422 g, 0.634 mmol) in diethyl ether (5 mL) was added ^tBuNC (71.7 μL, 0.634 mmol), all at room temperature. A color change from lime green to orange was

observed, and the solution was stirred for 15 min. Volatiles were then removed under reduced pressure to afford **18** as an orange powder. The resultant orange solid was recrystallized from a saturated pentane (5 mL) solution at $-30\text{ }^{\circ}\text{C}$, filtered, and dried in vacuo. Yield: 0.292 g (61%). Diffraction-quality crystals were grown from a saturated pentane solution at $-30\text{ }^{\circ}\text{C}$. ^1H NMR (toluene- d_8 , 299.9 MHz, 208 K): δ 7.14–6.89 (5 H, m, overlapping o - C_6H_5 , m - C_6H_5 , and p - C_6H_5), 3.31 (1 H, app sept, app $^3J = 6.3$ Hz, NCH_aMeMe), 3.17 (1 H, app sept, app $^3J = 6.3$ Hz, NCH_bMeMe), 2.30 (15 H, s, C_5Me_5), 1.52 (9 H, s, NOCMe_3), 1.07 (6 H, d, overlapping NCH_aMeMe and NCH_bMeMe), 1.04 (9 H, s, NCMe_3), 0.96 (3 H, d, $^3J = 6.3$ Hz, NCH_aMeMe), 0.91 (3 H, d, $^3J = 6.3$ Hz, NCH_bMeMe) ppm. $^{13}\text{C}\{^1\text{H}\}$ NMR (toluene- d_8 , 75.4 MHz, 208 K): δ 172.3 (PhCN $_2$), 153.8 (TiCN $_2$), 149.4 (NC(Ar $^{\text{F}_3}$)N), 135.1 (i - C_6H_5), 129.1–127.0 (overlapping with solvent, p - C_6H_5 , m - C_6H_5 , and o - C_6H_5), 118.3 (C_5Me_5), 114.1 (1 C, t, $^2J_{\text{C-F}} = 23.0$ Hz, i - C_6F_5), 77.4 (NOCMe $_3$), 55.9 (CNMe $_3$), 49.3 (NCH $_b\text{MeMe}$), 48.8 (NCH $_a\text{MeMe}$), 29.1 (CNMe $_3$), 27.9 (NOCMe $_3$), 26.3 (NCH $_b\text{MeMe}$), 25.7 (NCH $_a\text{MeMe}$), 25.2, 24.9 (NCH $_a\text{MeMe}$ and NCH $_b\text{MeMe}$), 12.7 (C_5Me_5) ppm. ^{13}C NMR (HMQC ^{19}F -observed, toluene- d_8 , 282.1 MHz, 208 K): δ 143.2 (o - C_6F_5), 142.9 (o - C_6F_5), 139.9 (p - C_6F_5), 137.5 (m - C_6F_5), 137.2 (m - C_6F_5) ppm. $^{19}\text{F}\{^1\text{H}\}$ NMR (toluene- d_8 , 282.1 MHz, 208 K): δ -138.5 (1 F, m, o - C_6F_5), -141.4 (1 F, m, o - C_6F_5), -158.1 (1 F, t, $^3J = 21.4$ Hz, p - C_6F_5), -163.8 (1 F, m, m - C_6F_5), -164.1 (1 F, m, m - C_6F_5) ppm. IR (NaCl plates, Nujol mull, cm^{-1}): 2186 (s), 1648 (m), 1576 (w), 1519 (s), 1499 (s), 1486 (s), 1368 (s), 1357 (s), 1336 (s), 1309 (m), 1292 (m), 1257 (m), 1239 (w), 1231 (w), 1194 (s), 1169 (m), 1133 (m), 1106 (m), 1075 (w), 1030 (m), 1008 (m), 990 (s), 981 (s), 973 (s), 937 (s), 917 (m), 892 (m), 860 (w), 810 (w), 792 (w), 781 (m), 739 (w), 719 (m), 706 (m), 670 (m), 607 (m), 595 (w), 580 (m). EI-MS: m/z 666 [$\text{M} - \text{BuNC}$] $^+$ (70%). Anal. Found (calcd for $\text{C}_{39}\text{H}_{52}\text{F}_5\text{N}_5\text{OTi}$): C, 62.57 (62.48); H, 7.13 (6.99); N, 9.24 (9.34).

Cp*Ti{PhC(N i Pr) $_2$ }{NC(NO i Bu)C $_6$ H $_4$ N(C $_6$ H $_3$ Me $_2$)C $_3$ (F)} (20). To a solution of Cp*Ti{PhC(N i Pr) $_2$ }{NC(Ar $^{\text{F}_3}$)NO i Bu} (5; 0.493 g, 0.739 mmol) in diethyl ether (2 mL) was added XylNC (97.0 mg, 0.739 mmol) in diethyl ether (2 mL), all at room temperature. A color change from lime green to red-orange was observed, and the solution was stirred for 16 h. Volatiles were then removed under reduced pressure to afford **20** as an orange powder which was dried in vacuo. Yield: 0.501 g (85%). Diffraction-quality crystals were grown from a saturated n -hexane solution at $-4\text{ }^{\circ}\text{C}$. ^1H NMR (toluene- d_8 , 299.9 MHz, 253 K): δ 7.12–6.87 (7 H, m, overlapping o - C_6H_5 , m - C_6H_5 , p - C_6H_5 , m - $\text{C}_6\text{H}_3\text{Me}_2$, and p - $\text{C}_6\text{H}_3\text{Me}_2$), 6.07 (1 H, d, $^3J = 7.5$ Hz, o - C_6H_5), 3.69 (1 H, app sept, app $^3J = 6.6$ Hz, NCH_aMeMe), 2.46 (3 H, s, $2,6$ - $\text{C}_6\text{H}_3\text{Me}_2\text{Me}_b$), 2.36 (15 H, s, C_5Me_5), 1.98 (3 H, s, $2,6$ - $\text{C}_6\text{H}_3\text{Me}_2\text{Me}_b$), 1.48 (9 H, s, NOCMe_3), 1.05 (3 H, d, $^3J = 6.3$ Hz, NCH_aMeMe), 1.00 (3 H, d, $^3J = 6.6$ Hz, NCH_bMeMe), 0.88 (3 H, d, $^3J = 6.9$ Hz, NCH_bMeMe), 0.68 (3 H, d, $^3J = 6.6$ Hz, NCH_bMeMe) ppm. $^{13}\text{C}\{^1\text{H}\}$ NMR (toluene- d_8 , 75.4 MHz, 253 K): δ 216.7 (Ti-NC), 170.4 (PhCN $_2$), 141.7 (1 C, d, $J = 3.1$ Hz, i - $\text{C}_6\text{H}_3\text{Me}_2$), 139.6 (br s, NC(Ar $^{\text{F}_3}$)N), 138.8 (1 C, d, $J = 4.2$ Hz, o - $\text{C}_6\text{H}_3\text{Me}_2$), 136.1 (i - C_6H_3), 135.2 (1 C, d, $J = 4.1$ Hz, o - $\text{C}_6\text{H}_3\text{Me}_2$), 129.6 (m - $\text{C}_6\text{H}_3\text{Me}_2$), 129.1–127.3 (overlapping with toluene- d_8 , o - C_6H_5 , o - C_6H_5 , m - C_6H_5 , p - C_6H_5 , and p - $\text{C}_6\text{H}_3\text{Me}_2$), 127.7 (m - $\text{C}_6\text{H}_3\text{Me}_2$), 126.4 (C_5Me_5), 103.0 (1 C, dd, $^2J_{\text{C-F}} = 18.7$ Hz, $^3J_{\text{C-F}} = 3.2$ Hz, Ti{NC(NO i Bu)C $_3$ }), 79.6 (NOCMe $_3$), 49.4 (NCH $_a\text{MeMe}$), 48.7 (NCH $_b\text{MeMe}$), 27.7 (overlapping NOCMe $_3$ and NCH $_a\text{MeMe}$), 25.2 (NCH $_a\text{MeMe}$), 25.0 (NCH $_b\text{MeMe}$), 25.0 (NCH $_b\text{MeMe}$), 19.0 (1 C, br d, $2,6$ - $\text{C}_6\text{H}_3\text{Me}_2\text{Me}_b$), 18.2 ($2,6$ - $\text{C}_6\text{H}_3\text{Me}_2\text{Me}_b$), 12.7 (C_5Me_5) ppm. The resonance attributed to Ti{CN(Xyl)C $_3$ } could not be observed. ^{13}C NMR (HMQC ^{19}F -observed, toluene- d_8 , 282.1 MHz, 253 K): δ 144.2 (inner $_1$ - $\text{C}_6\text{F}_4\text{N}$), 142.5 (inner $_2$ - $\text{C}_6\text{F}_4\text{N}$), 137.6 (outer $_1$ - $\text{C}_6\text{F}_4\text{N}$), 135.9 (outer $_3$ - $\text{C}_6\text{F}_4\text{N}$) ppm. $^{19}\text{F}\{^1\text{H}\}$ NMR (toluene- d_8 , 282.1 MHz, 253 K): δ -101.8 (1 F, br s, Ti-F), -118.7 (1 F, dt, $J = 24.8$ Hz, $J = 8.7$ Hz, inner $_1$ - $\text{C}_6\text{F}_4\text{N}$), -152.4 (1 F, td, $J = 22.0$, $J = 7.6$ Hz, inner $_2$ - $\text{C}_6\text{F}_4\text{N}$), -155.2 (1 F, dd, $J = 22.3$, $J = 22.0$, outer $_3$ - $\text{C}_6\text{F}_4\text{N}$), -162.7 (1 F, dd, $J = 21.7$, $J = 21.7$ Hz, outer $_4$ - $\text{C}_6\text{F}_4\text{N}$) ppm. IR (NaCl plates, Nujol mull, cm^{-1}): 2118 (w), 1638 (w), 1586 (w), 1511 (s), 1488 (s), 1366 (s), 1340 (m), 1328 (m), 1276 (w), 1258 (m), 1231 (w), 1218 (m), 1199

(m), 1190 (m), 1166 (w), 1146 (m), 1121 (w), 1100 (m), 1090 (m), 1038 (m), 1018 (m), 981 (s), 919 (w), 908 (m), 887 (m), 804 (w), 787 (w), 771 (m), 722 (w), 711 (m), 547 (w). EI-MS: m/z (calcd for $[\text{C}_{43}\text{H}_{52}\text{F}_5\text{N}_5\text{OTi}]^+$): 797.3562 (797.3576) (2%). Anal. Found (calcd for $\text{C}_{43}\text{H}_{52}\text{F}_5\text{N}_5\text{OTi}$): C, 64.86 (64.74); H, 6.45 (6.57); N, 8.81 (8.78).

NMR Tube Scale Synthesis of Cp*Ti{PhC(N i Pr) $_2$ }{N(B(Ar $^{\text{F}_3}$) $_3$)C(Ar $^{\text{F}_3}$)N(O i Bu)} (25). To a solution of Cp*Ti{PhC(N i Pr) $_2$ }{NC(Ar $^{\text{F}_3}$)NO i Bu} (5; 14.1 mg, 0.0211 mmol) in C_6D_6 (0.3 mL) in an NMR tube equipped with a J. Young Teflon valve was added B(Ar $^{\text{F}_3}$) $_3$ (12.5 mg, 0.0422 mmol) in C_6D_6 (0.3 mL) at room temperature. The reaction was monitored by ^1H , ^{19}F , and ^{11}B NMR spectroscopy. After ca. 7 h Cp*Ti{PhC(N i Pr) $_2$ }{N(B(Ar $^{\text{F}_3}$) $_3$)C(Ar $^{\text{F}_3}$)N(O i Bu)} (25) was formed alongside Cp*Ti{PhC(N i Pr) $_2$ }{ON(B(Ar $^{\text{F}_3}$) $_3$)C(Ar $^{\text{F}_3}$)N(H)-(B(Ar $^{\text{F}_3}$) $_3$)} (26) in a 86:14 ratio. 25 was characterized by ^1H , ^{19}F , and ^{11}B NMR spectroscopy. ^1H NMR (C_6D_6 , 299.9 MHz, 293 K): δ 7.40 (1 H, d, $^3J = 7.8$ Hz, o - C_6H_5), 7.12–6.91 (4 H, m, o - C_6H_5 , m - C_6H_5 , and p - C_6H_5), 3.38 (2 H, sept, $^3J = 6.6$ Hz, NCHMeMe), 2.19 (15 H, s, C_5Me_5), 1.46 (9 H, s, NOCMe $_3$), 0.80 (6 H, d, $^3J = 6.6$ Hz, NCHMeMe), 0.76 (6 H, d, $^3J = 6.3$ Hz, NCHMeMe) ppm. $^{19}\text{F}\{^1\text{H}\}$ NMR (C_6D_6 , 282.1 MHz, 293 K): δ -126.7 (m), -130.6 (6 F, br s, B(Ar $^{\text{F}_3}$) $_3$), -132.2 (m), -142.2 (3 F, m, B(Ar $^{\text{F}_3}$) $_3$), -145.6 (br s), -154.6 (m), -158.4 (t), -160.8 (6 F, br s, B(Ar $^{\text{F}_3}$) $_3$), -163.9 (m) ppm. ^{11}B NMR (C_6D_6 , 96.2 MHz, 293 K): δ -7 (B(Ar $^{\text{F}_3}$) $_3$) ppm.

Cp*Ti{PhC(N i Pr) $_2$ }{ON(B(Ar $^{\text{F}_3}$) $_3$)C(Ar $^{\text{F}_3}$)N(H)(B(Ar $^{\text{F}_3}$) $_3$)} (26). To a solution of Cp*Ti{PhC(N i Pr) $_2$ }{NC(Ar $^{\text{F}_3}$)NO i Bu} (5; 0.282 g, 0.422 mmol) in benzene (5 mL) was added a solution of B(Ar $^{\text{F}_3}$) $_3$ (0.250 g, 0.845 mmol) in benzene (5 mL), all at room temperature. A color change from lime green to dark green was observed, and the solution was heated to $70\text{ }^{\circ}\text{C}$ and stirred for 4 days. Volatiles were then removed under reduced pressure to afford **26** as a dark green oily solid. The resultant green solid was washed with pentane (3 \times 5 mL, room temperature), filtered, and dried in vacuo. Yield: 0.362 g (76%). The resultant green powder was subsequently washed with diethyl ether (1 \times 5 mL, room temperature), filtered, and dried in vacuo to give an analytically pure sample. Yield: 0.124 g (26%). ^1H NMR (CD_2Cl_2 , 499.9 MHz, 293 K): δ 7.52–7.47 (4 H, m, overlapping o - C_6H_5 , m - C_6H_5 , and p - C_6H_5), 7.33 (1 H, m, o - C_6H_5), 6.67 (1 H, s, NH), 3.46 (2 H, 2 \times app sept, app $^3J = 6.5$ Hz, overlapping NCH $_a\text{MeMe}$ and NCH $_b\text{MeMe}$), 2.02 (15 H, s, C_5Me_5), 0.98 (3 H, d, $^3J = 6.5$ Hz, NCH $_a\text{MeMe}$), 0.93 (3 H, d, $^3J = 7.0$ Hz, NCH $_b\text{MeMe}$), 0.83 (3 H, d, $^3J = 6.5$ Hz, NCH $_b\text{MeMe}$), 0.82 (3 H, d, $^3J = 7.0$ Hz, NCH $_b\text{MeMe}$) ppm. $^{13}\text{C}\{^1\text{H}\}$ NMR (CD_2Cl_2 , 125.7 MHz, 293 K): δ 167.1 (PhCN $_2$), 153.0 (NC(Ar $^{\text{F}_3}$)N), 148.9 (2 C, br d, $^1J_{\text{C-F}} = 235.0$ Hz, o - C_6F_5), 145.7 (2 C, d, $^1J_{\text{C-F}} = 245.9$ Hz, o - C_6F_5), 144.5 (1 C, d, $^1J_{\text{C-F}} = 251.2$ Hz, p - C_6F_5), 143.1 (2 C, d, $^1J_{\text{C-F}} = 257.1$ Hz, m - C_6F_5), 139.9 (1 C, d, $^1J_{\text{C-F}} = 248.0$ Hz, p - C_6F_5), 137.2 (2 C, d, $^1J_{\text{C-F}} = 246.8$ Hz, m - C_6F_5), 132.4 (i - C_6H_5), 131.1 (C_5Me_5), 129.9, 129.1, 129.0, 128.9 (o - C_6H_5 , o - C_6H_5 , m - C_6H_5 , and p - C_6H_5), 128.5 (1 C, br s, i - C_6F_5), 108.9 (1 C, app t, $^2J_{\text{C-F}} = 19.6$ Hz, i - C_6F_5), 52.1 (NCH $_a\text{MeMe}$), 51.1 (NCH $_b\text{MeMe}$), 26.1 (NCH $_b\text{MeMe}$), 25.4 (NCH $_a\text{MeMe}$), 25.4 (NCH $_a\text{MeMe}$), 24.2 (NCH $_b\text{MeMe}$), 13.1 (C_5Me_5) ppm. $^{19}\text{F}\{^1\text{H}\}$ NMR (CD_2Cl_2 , 282.1 MHz, 293 K): δ -132.5 (br s), -133.2 (2 F, br s, o - C_6F_5), -134.2 (br s), -135.7 (2 F, br m, o - C_6F_5), -135.8 (br m), -136.6 (br s), 150.1 (1 F, t of t, $^3J = 20.6$, $^4J = 3.7$ Hz, p - C_6F_5), -158.1 (br s), -160.7 (br s), -161.5 (1 F, t of d, $^3J = 21.6$, $^4J = 8.2$ Hz, m - C_6F_5), -162.5 (1 F, t of d, $^3J = 21.6$, $^4J = 7.3$ Hz, m - C_6F_5), -166.0 (br m, m - C_6F_5), 166.8 (br s) ppm. ^{11}B NMR (CD_2Cl_2 , 96.2 MHz, 293 K): δ -7.1 (B(Ar $^{\text{F}_3}$) $_3$) ppm. ^1H NMR (CD_2Cl_2 , 299.9 MHz, 213 K): δ 7.46 (4 H, br s, overlapping o - C_6H_5 , m - C_6H_5 , and p - C_6H_5), 7.30 (1 H, br m, o - C_6H_5), 6.65 (1 H, s, NH), 3.35 (2 H, 2 \times br m, overlapping NCH $_a\text{MeMe}$ and NCH $_b\text{MeMe}$), 1.90 (15 H, s, C_5Me_5), 0.91 (3 H, br d, NCH $_a\text{MeMe}$), 0.84 (3 H, d, $^3J = 7.0$ Hz, NCH $_a\text{MeMe}$), 0.73 (6 H, br m, overlapping NCH $_b\text{MeMe}$ and NCH $_b\text{MeMe}$) ppm. $^{19}\text{F}\{^1\text{H}\}$ NMR (CD_2Cl_2 , 282.1 MHz, 213 K): δ -121.5 (br s), -126.2 (br, t), -126.8 (br, t), -131.6 (br, t), -132.6 (br m), -132.9 (br d), -133.7 (br m), -134.3 (br d), -135.9 (br d), -139.6 (br s), -149.4 (1 F, t, $^3J = 21.2$, p_1 - C_6F_5), -156.9 (1 F, t, $^3J = 21.7$, p_2 - C_6F_5), -159.8 (1 F, t, $^3J = 21.4$, p_3 - C_6F_5), -160.5 (1 F, t, $^3J = 21.4$, p_4 - C_6F_5), -161.4 (1 F, app t, m_{1a} - C_6F_5), -161.8 (1 F, app t, m_{1b} - C_6F_5), -162.8 (1 F, app t, m_{2a} - C_6F_5), -165.0 (1 F, app t, m_{4a} - C_6F_5), -166.1 (1 F, app t, m_{3a} - C_6F_5), -166.3 (1 F, app

t, m_{4b} -C₆F₅), -166.6 (1 F, app t, m_{2b} -C₆F₅), -167.0 (1 F, app t, m_{3b} -C₆F₅) ppm. At this temperature the resonance attributed to B(Ar^{F5})₃ in the ¹¹B NMR spectrum could not be identified. IR (NaCl plates, Nujol mull, cm⁻¹): 3393 (w), 1642 (m), 1517 (s), 1504 (m), 1406 (m), 1334 (m), 1278 (w), 1261 (w), 1221 (w), 1096 (m), 1018 (m), 1000 (m), 979 (m), 864 (w), 812 (m), 782 (m), 766 (w), 749 (w), 707 (w), 695 (w), 687 (w), 679 (w), 659 (w), 615 (m), 596 (m). EI-MS: m/z 610 [Cp*Ti{PhC(NⁱPr)₂}{ONC(Ar^{F5})N(H)}], $M - 2B$ -(Ar^{F5})₃⁺ (5%). Anal. Found (calcd for C₆₆H₃₅B₂F₃₅N₄O₂Ti): C, 48.59 (48.50); H, 2.23 (2.16); N, 3.48 (3.43).

Crystal Structure Determinations. Crystal data collection and processing parameters for Cp*Ti{PhC(NⁱPr)₂}{NC(Ar^{F5})NO^tBu}C(Ph)(H)O} (13a), (4-C₆H₄NMe₂)C{NC(Ar^{F5})NO^tBu}H (14e), Me₂NC{NC(Ar^{F5})NO^tBu}H (16), Cp*Ti{PhC(NⁱPr)₂}{NC(Ar^{F5})NO^tBu}('BuNC) (18), and Cp*Ti{PhC(NⁱPr)₂}{NC(NO^tBu)-C₆F₄N(C₆H₃Me₂)C}(F) (20) are given in Table S5 of the Supporting Information. Crystals were mounted on glass fibers using perfluoropolyether oil and cooled rapidly under a stream of cold N₂ using an Oxford Cryosystems Cryostream unit. Diffraction data were measured using either an Enraf-Nonius KappaCCD or Agilent Technologies Supernova diffractometer with Mo K α or Cu K α radiation, respectively. As appropriate, absorption and decay corrections were applied to the data and equivalent reflections merged.⁴² The structures were solved with SIR92⁴³ or Superflip,⁴⁴ and further refinements and all other crystallographic calculations were performed using the CRYSTALS program suite.⁴⁵ Other details of the structure solution and refinements are given in the Supporting Information. A full listing of atomic coordinates, bond lengths and angles, and displacement parameters for all of the structures have been deposited at the Cambridge Crystallographic Data Centre.

Computational Details. DFT calculations were carried out using the Amsterdam Density Functional program suite ADF 2013.01.⁴⁶ The generalized gradient approximation was employed, using the local density approximation of Vosko, Wilk, and Nusair⁴⁷ together with nonlocal exchange corrections by Becke⁴⁸ and nonlocal correlation corrections by Perdew.⁴⁹ TZP basis sets were used with triple- ζ accuracy sets of Slater-type orbitals and a polarization function added to the main-group atoms. The default SCF convergence criteria were used, together with a "good" Becke integration grid. The cores of the atoms were frozen up to 1s for C, N, O, and F. Full optimization of geometry was performed without any symmetry constraint, followed by analytical computation of the Hessian matrix to identify the nature of the located extrema as minima or transition states.

■ ASSOCIATED CONTENT

Supporting Information

Text, tables, figures, and CIF files giving general experimental procedures and details of starting materials, remaining details of the synthesis and characterization data for new compounds, further details of the DFT calculations and crystal structure determinations, including X-ray data collection and processing parameters and further data. This material is available free of charge via the Internet at <http://pubs.acs.org>.

■ AUTHOR INFORMATION

Corresponding Author

*E-mail for P.M.: philip.mountford@chem.ox.ac.uk.

Notes

The authors declare no competing financial interest.

■ ACKNOWLEDGMENTS

We thank Wolfson College, Oxford, U.K., for a Junior Research Fellowship to A.D.S., the Department of Chemistry, University of Oxford, Oxford, U.K., for a scholarship to L.R.G., and LANXESS Elastomers for a studentship to A.F.R.

■ REFERENCES

- (1) (a) Wigley, D. E. *Prog. Inorg. Chem.* **1994**, *42*, 239. (b) Duncan, A. P.; Bergman, R. G. *The Chemical Record* **2002**, *2*, 431. (c) Mountford, P. *Chem. Commun.* **1997**, 2127. (d) Gade, L. H.; Mountford, P. *Coord. Chem. Rev.* **2001**, *216–217*, 65. (e) Hazari, N.; Mountford, P. *Acc. Chem. Res.* **2005**, *38*, 839. (f) Fout, A. R.; Kilgore, U. J.; Mindiola, D. J. *Chem. Eur. J.* **2007**, *13*, 9428. (g) Kozak, C. M.; Mountford, P. *Angew. Chem., Int. Ed.* **2004**, *43*, 1186.
- (2) (a) Wiberg, N.; Haring, H.-W.; Huttner, G.; Friedrich, P. *Chem. Ber.* **1978**, *111*, 2708. (b) Blake, A. J.; McInnes, J. M.; Mountford, P.; Nikonov, G. L.; Swallow, D.; Watkin, D. J. *Chem. Soc., Dalton Trans.* **1999**, 379. (c) Thorman, J. L.; Woo, L. K. *Inorg. Chem.* **2000**, *39*, 1301. (d) Li, Y.; Shi, Y.; Odom, A. L. *J. Am. Chem. Soc.* **2004**, *126*, 1794. (e) Banerjee, S.; Shi, Y.; Cao, C.; Odom, A. L. *J. Organomet. Chem.* **2005**, *690*, 5066. (f) Parsons, T. B.; Hazari, N.; Cowley, A. R.; Green, J. C.; Mountford, P. *Inorg. Chem.* **2005**, *44*, 8442. (g) Banerjee, S.; Odom, A. L. *Organometallics* **2006**, *25*, 3099. (h) Patel, S.; Li, Y.; Odom, A. L. *Inorg. Chem.* **2007**, *46*, 6373. (i) Selby, J. D.; Manley, C. D.; Feliz, M.; Schwarz, A. D.; Clot, E.; Mountford, P. *Chem. Commun.* **2007**, 4937. (j) Banerjee, S.; Barnea, E.; Odom, A. L. *Organometallics* **2008**, *27*, 1005. (k) Clulow, A. J.; Selby, J. D.; Cushion, M. G.; Schwarz, A. D.; Mountford, P. *Inorg. Chem.* **2008**, *47*, 12049. (l) Selby, J. D.; Manley, C. D.; Schwarz, A. D.; Clot, E.; Mountford, P. *Organometallics* **2008**, *27*, 6479. (m) Selby, J. D.; Schulten, C.; Schwarz, A. D.; Stasch, A.; Clot, E.; Jones, C.; Mountford, P. *Chem. Commun.* **2008**, 5101. (n) Weitershaus, K.; Fillol, J. L.; Wadepohl, H.; Gade, L. H. *Organometallics* **2009**, *28*, 4747. (o) Weitershaus, K.; Wadepohl, H.; Gade, L. H. *Organometallics* **2009**, *28*, 3381. (p) Janssen, T.; Severin, R.; Diekmann, M.; Friedemann, M.; Haase, D.; Saak, W.; Doye, S.; Beckhaus, R. *Organometallics* **2010**, *29*, 1806. (q) Schofield, A. D.; Nova, A.; Selby, J. D.; Manley, C. D.; Schwarz, A. D.; Clot, E.; Mountford, P. *J. Am. Chem. Soc.* **2010**, *132*, 10484. (r) Tiong, P. J.; Schofield, A. D.; Selby, J. D.; Nova, A.; Clot, E.; Mountford, P. *Chem. Commun.* **2010**, *46*, 85. (s) Schofield, A. D.; Nova, A.; Selby, J. D.; Schwarz, A. D.; Clot, E.; Mountford, P. *Chem. Eur. J.* **2011**, *17*, 265. (t) Selby, J. D.; Feliz, M.; Schwarz, A. D.; Clot, E.; Mountford, P. *Organometallics* **2011**, *30*, 2295. (u) Tiong, P. J.; Nova, A.; Clot, E.; Mountford, P. *Chem. Commun.* **2011**, *47*, 3147. (v) Tiong, P. J.; Nova, A.; Groom, L. R.; Schwarz, A. D.; Selby, J. D.; Schofield, A. D.; Clot, E.; Mountford, P. *Organometallics* **2011**, *30*, 1182. (w) Schwarz, A. D.; Onn, C. S.; Mountford, P. *Angew. Chem., Int. Ed.* **2012**, *51*, 12298. (x) Tiong, P. J.; Nova, A.; Schwarz, A. D.; Selby, J. D.; Clot, E.; Mountford, P. *Dalton Trans.* **2012**, *41*, 2277. (y) Schweitzer, P. D.; Wadepohl, H.; Gade, L. H. *Organometallics* **2013**, *32*, 3697–3709. (z) Unruangsri, J.; Morgan, H.; Schwarz, A. D.; Schofield, A. D.; Mountford, P. *Organometallics* **2013**, *32*, 3091–3107.
- (3) (a) Walsh, P. J.; Carney, M. J.; Bergman, R. G. *J. Am. Chem. Soc.* **1991**, *113*, 6343. (b) Herrmann, H.; Fillol, J. L.; Wadepohl, H.; Gade, L. H. *Angew. Chem., Int. Ed.* **2007**, *46*, 8426. (c) Herrmann, H.; Fillol, J. L.; Gehrman, T.; Enders, M.; Wadepohl, H.; Gade, L. H. *Chem. Eur. J.* **2008**, *14*, 8131. (d) Herrmann, H.; Fillol, J. L.; Wadepohl, H.; Gade, L. H. *Organometallics* **2008**, *27*, 172. (e) Herrmann, H.; Gehrman, T.; Wadepohl, H.; Gade, L. H. *Dalton Trans.* **2008**, 6231. (f) Herrmann, H.; Wadepohl, H.; Gade, L. H. *Dalton Trans.* **2008**, 2111. (g) Gehrman, T.; Fillol, J. L.; Wadepohl, H.; Gade, L. H. *Angew. Chem., Int. Ed.* **2009**, *48*, 2152. (h) Munha, R. F.; Veiros, L. F.; Duarte, M. T.; Fryzuk, M. D.; Martins, A. M. *Dalton Trans.* **2009**, 7494. (i) Gehrman, T.; Fillol, J. L.; Wadepohl, H.; Gade, L. H. *Organometallics* **2010**, *29*, 28. (j) Gehrman, T.; Fillol, J. L.; Scholl, S. A.; Wadepohl, H.; Gade, L. H. *Angew. Chem., Int. Ed.* **2011**, *50*, 5757. (k) Gehrman, T.; Fillol, J. L.; Wadepohl, H.; Gade, L. H. *Organometallics* **2012**, *31*, 4504. (l) Gehrman, T.; Kruck, M.; Wadepohl, H.; Gade, L. H. *Chem. Commun.* **2012**, *48*, 2397. (m) Gehrman, T.; Plundrich, G. T.; Wadepohl, H.; Gade, L. H. *Organometallics* **2012**, *31*, 3346–3354. (n) Gehrman, T.; Scholl, S. A.; Fillol, J. L.; Wadepohl, H.; Gade, L. H. *Chem. Eur. J.* **2012**, *18*, 3925. (o) Scholl, S. A.; Plundrich, G. T.; Wadepohl, H.; Gade, L. H. *Inorg. Chem.* **2013**, *52*, 10158–10166. (p) Scholl, S. A.; Wadepohl, H.; Gade, L. H. *Organometallics* **2013**, *32*, 937–940.

- (4) (a) Cundari, T. R. *J. Am. Chem. Soc.* **1992**, *114*, 7879. (b) Lin, Z.; Hall, M. B. *Coord. Chem. Rev.* **1993**, *123*, 149. (c) Mountford, P.; Swallow, D. J. *Chem. Soc., Chem. Commun.* **1995**, 2357. (d) Kaltsoyannis, N.; Mountford, P. *J. Chem. Soc., Dalton Trans.* **1999**, 781. (e) Cundari, T. R. *Chem. Rev.* **2000**, *100*, 807. (f) Schwarz, A. D.; Nielson, A. J.; Kaltsoyannis, N.; Mountford, P. *Chem. Sci.* **2012**, *3*, 819. (g) Tiong, P. J.; Groom, L. R.; Clot, E.; Mountford, P. *Chem. Eur. J.* **2013**, *19*, 4198.
- (5) (a) Adams, N.; Arts, H. J.; Bolton, P. D.; Cowell, D.; Dubberley, S. R.; Friederichs, N.; Grant, C.; Kranenburg, M.; Sealey, A. J.; Wang, B.; Wilson, P. J.; Cowley, A. R.; Mountford, P.; Schröder, M. *Chem. Commun.* **2004**, 434. (b) Bolton, P. D.; Mountford, P. *Adv. Synth. Catal.* **2005**, *347*, 355. (c) Bigmore, H. R.; Dubberley, S. R.; Kranenburg, M.; Lawrence, S. C.; Sealey, A. J.; Selby, J. D.; Zuideveld, M.; Cowley, A. R.; Mountford, P. *Chem. Commun.* **2006**, 436. (d) Bigmore, H. R.; Zuideveld, M.; Kowalczyk, R. M.; Cowley, A. R.; Kranenburg, M.; McInnes, E. J. L.; Mountford, P. *Inorg. Chem.* **2006**, *45*, 6411. (e) Wilson, P. J.; Blake, A. J.; Mountford, P.; Schröder, M. *Chem. Commun.* **1998**, 1007.
- (6) van Asselt, A.; Santarsiero, B. D.; Bercaw, J. E. *J. Am. Chem. Soc.* **1986**, *108*, 8291.
- (7) (a) Schwarz, A. D.; Nova, A.; Clot, E.; Mountford, P. *Chem. Commun.* **2011**, 47, 4926. (b) Schwarz, A. D.; Nova, A.; Clot, E.; Mountford, P. *Inorg. Chem.* **2011**, *50*, 12155. (c) Groom, L. R.; Schwarz, A. D.; Nova, A.; Clot, E.; Mountford, P. *Organometallics* **2013**, *32*, 7520–7539.
- (8) (a) Stevens, R. E.; Gladfelter, W. L. *J. Am. Chem. Soc.* **1982**, *104*, 6454. (b) Haug, K.; Hiller, W.; Strähle, J. Z. *Anorg. Allg. Chem.* **1986**, *533*, 49. (c) Green, M. L. H.; James, J. T.; Sanders, J. F. *Chem. Commun.* **1996**, 1343. (d) Sharp, W. B.; Daff, P. J.; McNeil, W. S.; Legzdins, P. *J. Am. Chem. Soc.* **2001**, *123*, 6272. (e) Arashiba, K.; Matsukawa, S.; Kuwata, S.; Tanabe, Y.; Iwasaki, M.; Ishii, Y. *Organometallics* **2006**, *25*, 560. (f) Lee, K. K.-H.; Wong, W. T. *J. Organomet. Chem.* **1999**, *577*, 323.
- (9) (a) Guiducci, A. E.; Cowley, A. R.; Skinner, M. E. G.; Mountford, P. *J. Chem. Soc., Dalton Trans.* **2001**, 1392. (b) Boyd, C. L.; Guiducci, A. E.; Dubberley, S. R.; Tyrrell, B. R.; Mountford, P. *J. Chem. Soc., Dalton Trans.* **2002**, 4175. (c) Boyd, C. L.; Clot, E.; Guiducci, A. E.; Mountford, P. *Organometallics* **2005**, *24*, 2347. (d) Guiducci, A. E.; Boyd, C. L.; Mountford, P. *Organometallics* **2006**, *25*, 1167. (e) Guiducci, A. E.; Boyd, C. L.; Clot, E.; Mountford, P. *Dalton Trans.* **2009**, 5960.
- (10) (a) Chisholm, M. H.; Delbridge, E. E.; Kidwell, A. R.; Quinlan, K. B. *Chem. Commun.* **2003**, 126. (b) Gdula, R. L.; Johnson, M. J. A.; Ockwig, N. W. *Inorg. Chem.* **2005**, *44*, 9140.
- (11) (a) Wood, C. D.; McLain, S. J.; Schrock, R. R. *J. Am. Chem. Soc.* **1979**, *101*, 3210. (b) Schrock, R. R.; Fellmann, J. D. *J. Am. Chem. Soc.* **1978**, *100*, 3359. (c) Doxsee, K. M.; Farahi, J. B.; Hope, H. J. *Am. Chem. Soc.* **1991**, *113*, 8889. (d) Hessen, B.; Buijink, J.-K. F.; Meetsma, A.; Teuben, J.; Helgesson, G.; Hakansson, M.; Jagner, S.; Spek, A. L. *Organometallics* **1993**, *12*, 2268. (e) Basuli, F.; Aneetha, H.; Huffman, J. C.; Mendiola, D. J. *J. Am. Chem. Soc.* **2005**, *127*, 17992.
- (12) (a) Litemann, M. L.; Schrock, R. R. *Organometallics* **1985**, *4*, 74. (b) Freudenberger, J. H.; Schrock, R. R. *Organometallics* **1986**, *5*, 398. (c) Chisholm, M. H.; Folting, K.; Lynn, M. L.; Tiedtke, D. B.; Lemoigno, F.; Eisenstein, O. *Chem. Eur. J.* **1999**, *5*, 2318. (d) Geyer, A. M.; Gdula, R. L.; Wiedner, E. S.; Johnson, M. J. A. *J. Am. Chem. Soc.* **2007**, *129*, 3800. (e) Bailey, B. C.; Fout, A. R.; Fan, H.; Tomaszewski, J.; Huffman, J. C.; Gary, J. B.; Johnson, M. J. A.; Mendiola, D. J. *J. Am. Chem. Soc.* **2007**, *129*, 2234. (f) Geyer, A. M.; Wiedner, E. S.; Gary, J. B.; Gdula, R. L.; Kuhlmann, N. C.; Johnson, M. J. A.; Dunietz, B. D.; Kampf, J. W. *J. Am. Chem. Soc.* **2008**, *130*, 8984.
- (13) Pugh, S. M.; Trösch, D. J. M.; Wilson, D. J.; Bashall, A.; Cloke, F. G. N.; Gade, L. H.; Hitchcock, P. B.; McPartlin, M.; Nixon, J. F.; Mountford, P. *Inorg. Chem.* **2000**, *19*, 3205.
- (14) Carney, M. J.; Walsh, P. J.; Hollander, F. J.; Bergman, R. G. *Organometallics* **1992**, *11*, 761.
- (15) Glueck, D. S.; Wu, J.; Hollander, F. J.; Bergman, R. G. *J. Am. Chem. Soc.* **1991**, *113*, 2041.
- (16) Goerdeler, J.; Eggers, W. *Chem. Ber.* **1986**, *119*, 3737.
- (17) Lee, S. Y. *J. Am. Chem. Soc.* **1996**, *118*, 6396.
- (18) So, L.-C.; Liu, C.-C.; Chan, M. C. W.; Lo, J. C. Y.; Sze, K.-H.; Zhu, N. *Chem. Eur. J.* **2012**, *18*, 565.
- (19) Fletcher, D. A.; McMeeking, R. F.; Parkin, D. *J. Chem. Inf. Comput. Sci.* **1996**, *36*, 746 (the UK Chemical Database Service: CSD version 5.34 updated May 2013).
- (20) For leading references see: Adams, N.; Cowley, A. R.; Dubberley, S. R.; Sealey, A. J.; Skinner, M. E. G.; Mountford, P. *Chem. Commun.* **2001**, 2738.
- (21) Hansch, C.; Leo, A.; Taft, R. W. *Chem. Rev.* **1991**, *91*, 165.
- (22) Jordan, R. B. *Reaction Mechanisms of Inorganic and Organometallic Systems*; Oxford University Press: Oxford, U.K., 1998.
- (23) March, J. *Advanced Organic Chemistry*; 4th ed.; Wiley-Interscience: New York, 1992.
- (24) Gordon, A. J.; Ford, R. A. *The Chemist's Companion: A Handbook of Practical Data, Techniques and References*; Wiley: New York, 1973.
- (25) Time-dependent DFT (TD-DFT) calculations for **14a,e** confirmed that the first significant lowest energy bands correspond to the ${}^1A_{\text{HOMO}} \rightarrow {}^1A_{\text{LUMO}}$ transitions.
- (26) Lee, S. Y.; Bergman, R. G. *J. Am. Chem. Soc.* **1996**, *118*, 6396.
- (27) Allen, F. H.; Kennard, O.; Watson, D. G.; Brammer, L.; Orpen, A. G.; Taylor, R. *J. Chem. Soc., Perkin Trans. 2* **1987**, , 51.
- (28) Estimations of entropy using DFT can be subject to errors of at least 7 cal mol⁻¹ K⁻¹, giving variations in ΔS of ca. ± 2 kcal mol⁻¹ at 298 K: Ayala, P. Y.; Schlegel, H. B. *J. Chem. Phys.* **1988**, *108*, 2314. Watson, L. A.; Eisenstein, O. *J. Chem. Educ.* **2002**, *79*, 1269 and references therein. This is comparable to the calculated differences in ΔH between the conformers under consideration, and therefore we prefer to neglect the small differences in entropy between them in this case.
- (29) Walsh, P. J.; Hollander, F. J.; Bergman, R. G. *Organometallics* **1993**, *12*, 3705.
- (30) (a) Danopoulos, A. D.; Wilkinson, G.; Sweet, T. K. N.; Hursthouse, M. B. *J. Chem. Soc., Dalton Trans.* **1996**, 271. (b) Blake, A. J.; Collier, P. E.; Gade, L. H.; McPartlin, M.; Mountford, P.; Schubart, M.; Scowen, I. *J. Chem. Commun.* **1997**, 1555. (c) Bashall, A.; Collier, P. E.; Gade, L. H.; McPartlin, M.; Mountford, P.; Pugh, S. M.; Radojevic, S.; Schubart, M.; Scowen, I. J.; Trösch, D. J. M. *Organometallics* **2000**, *19*, 4784.
- (31) (a) Kaplan, A. W.; Polse, J. L.; Ball, G. E.; Andersen, R. A.; Bergman, R. G. *J. Am. Chem. Soc.* **1998**, *120*, 11649. (b) Dunn, S. C.; Hazari, N.; Cowley, A. R.; Green, J. C.; Mountford, P. *Organometallics* **2006**, *25*, 1755. (c) Tiong, P. J. D.Phil. Thesis, University of Oxford, 2012.
- (32) (a) Vogler, A. *Isonitrile Chemistry*; Academic Press: New York and London, 1971. (b) Carofiglio, T.; Floriani, C.; Chiesi-Villa, A.; Guastini, C. *Inorg. Chem.* **1989**, *28*, 4417. (c) Carofiglio, T.; Cozzi, P. G.; Floriani, C.; Chiesi-Villa, A.; Rizzoli, C. *Organometallics* **1993**, *12*, 2726. (d) Hahn, F. E.; Lügger, T. *J. Organomet. Chem.* **1995**, *501*, 341.
- (33) Floriani, C.; Corazza, F.; Lesueur, W.; Chiesi-Villa, A.; Guastini, C. *Angew. Chem., Int. Ed. Engl.* **1989**, *28*, 66.
- (34) Kiplinger, J. L.; Richmond, T. G.; Osterberg, C. E. *Chem. Rev.* **1994**, *94*, 373. Bexrud, J. A.; Li, C.; Schafer, L. L. *Organometallics* **2007**, *26*, 6366. Scholl, S. A.; Plundrich, G. T.; Wadepohl, H.; Gade, L. H. *Inorg. Chem.* **2013**, *52*, 10158.
- (35) (a) Sotoodeh, M.; Lechtweis, I.; Roesky, H. W.; Noltemeyer, M.; Schmidt, H.-G. *Chem. Ber.* **1993**, *126*, 913. (b) Winter, C. H.; Zhou, X. X.; Heeg, M. J. *Inorg. Chem.* **1992**, *31*, 1808. (c) Klahn, M.; Arndt, P.; Spannberg, A.; Gansaeuer, A.; Rosenthal, U. *Organometallics* **2008**, *27*, 5846. (d) Kickbusch, R.; Lentz, D. *Chem. Commun.* **2010**, 46, 2118.
- (36) Wang, Z.; Wang, M.; Yao, X.; Li, Y.; Tan, J.; Wang, L.; Qiao, W.; Geng, Y.; Liu, Y.; Wang, Q. *Eur. J. Med. Chem.* **2012**, *53*, 275.
- (37) Zhang, J.; Zhu, D.; Yu, C.; Wan, C.; Wang, Z. *Org. Lett.* **2010**, *12*, 2841.
- (38) Wang, C.; Li, S.; Liu, H.; Jiang, Y.; Fu, H. *J. Org. Chem.* **2010**, *75*, 7936.

- (39) Stobenau, E. J.; Jordan, R. F. *J. Am. Chem. Soc.* **2003**, *125*, 8162.
- (40) (a) Lian, B.; Toupet, L.; Carpentier, J.-F. *Chem. Eur. J.* **2004**, *10*, 4301. (b) Lian, B.; Lehmann, C. W.; Navarro, C.; Carpentier, J.-F. *Organometallics* **2005**, *24*, 2466.
- (41) Hermanek, S. *Chem. Rev.* **1992**, *92*, 325.
- (42) (a) Otwinowski, Z.; Minor, W. *Processing of X-ray Diffraction Data Collected in Oscillation Mode*; Academic Press: New York, 1997. (b) *CrysAlisPro*; Agilent Technologies, Oxford, U.K., 2011.
- (43) Altomare, A.; Casciaro, G.; Giacovazzo, G.; Guagliardi, A.; Burla, M. C.; Polidori, G.; Camalli, M. *J. Appl. Crystallogr.* **1994**, *27*, 435.
- (44) Palatinus, L.; Chapuis, G. *J. Appl. Crystallogr.* **2007**, *40*, 786.
- (45) Betteridge, P. W.; Cooper, J. R.; Cooper, R. I.; Prout, K.; Watkin, D. J. *J. Appl. Crystallogr.* **2003**, *36*, 1487.
- (46) (a) te Velde, G.; Bickelhaupt, F. M.; Van Gisbergen, S.; Fonseca Guerra, C.; Baerends, E. J.; Snijders, J. G.; Ziegler, T. *J. Comput. Chem.* **2001**, *22*, 931. (b) Fonseca Guerra, C.; Snijders, J. G.; te Velde, G.; Baerends, E. J. *Theo. Chem. Acc.* **1998**, *99*, 391. (c) Baerends, E. J.; Ziegler, T.; Autschbach, J.; Bashford, D.; Bérces, A.; Bickelhaupt, F. M.; Bo, C.; Boerrigter, P. M.; Cavallo, L.; Chong, D. P.; Deng, L.; Dickson, R. M.; Ellis, D. E.; van Faassen, M.; Fan, L.; Fischer, T. H.; Fonseca Guerra, C.; Franchini, M.; Ghysels, A.; Giammona, A.; van Gisbergen, S. J. A.; Götz, A. W.; Groeneveld, J. A.; Gritsenko, O. V.; Grüning, M.; Gusarov, S.; Harris, F. E.; van den Hoek, P.; Jacob, C. R.; Jacobsen, H.; Jensen, L.; Kaminski, J. W.; van Kessel, G.; Kootstra, F.; Kovalenko, A.; Krykunov, M. V.; van Lenthe, E.; McCormack, D. A.; Michalak, A.; Mitoraj, M.; Morton, S. M.; Neugebauer, J.; Nicu, V. P.; Noodleman, L.; Osinga, V. P.; Patchkovskii, S.; Pavanello, M.; Philipsen, P. H. T.; Post, D.; Pye, C. C.; Ravenek, W.; Rodríguez, J. I.; Ros, P.; Schipper, P. R. T.; Schreckenbach, G.; Seldenthuis, J. S.; Seth, M.; Snijders, J. G.; Solà, M.; Swart, M.; Swerhone, D.; te Velde, G.; Vernooijs, P.; Versluis, L.; Visscher, L.; Visser, O.; Wang, F.; Wesolowski, T. A.; van Wezenbeek, E. M.; Wiesenekker, G.; Wolff, S. K.; Woo, T. K.; Yakovlev, A. L. *ADF2013*; SCM, Theoretical Chemistry, Vrije Universiteit, Amsterdam, 2013; <http://www.scm.com>.
- (47) Vosko, S. H.; Wilk, L.; Nusair, M. *Can. J. Phys.* **1980**, *58*, 1200.
- (48) (a) Becke, A. D. *Phys. Rev. A* **1988**, *38*, 3098. (b) Becke, A. D. *J. Chem. Phys.* **1988**, *88*, 1053.
- (49) Perdew, J. P.; Yue, W. *Phys. Rev. B* **1986**, *33*, 8800.